AD NUMBER
AD481757
LIMITATION CHANGES
TO: **Approved for public release; distribution is unlimited.**
FROM: **Distribution authorized to U.S. Gov't. agencies and their contractors; Administrative/Operational Use; 1962. Other requests shall be referred to U.S. Naval Postgraduate School, Monterey, CA 93943.**
AUTHORITY
USNPS ltr, 18 Oct 1971

GAMMA-GAMMA ANGULAR CORRELATION IN NICKEL 60

BRUCE KENNEDY

GAMMA-GAMMA ANGULAR CORRELATION

IN NICKEL 60

* * * * *

Bruce Kennedy

GAMMA-GAMMA ANGULAR CORRELATION

IN NICKEL 60

by

Bruce Kennedy
//
Captain, United States Army

Submitted in partial fulfillment of
the requirements for the degree of

MASTER OF SCIENCE
IN
PHYSICS

United States Naval Postgraduate School
Monterey, California

1962

GAMMA-GAMMA ANGULAR CORRELATION IN NICKEL 60

by

Bruce Kennedy

This work is accepted as fulfilling
the thesis requirements for the degree of
MASTER OF SCIENCE
IN
PHYSICS
from the
United States Naval Postgraduate School

ABSTRACT

A reinvestigation was conducted of an anomaly in the experimental angular correlation for the gamma-gamma cascade of Ni^{60} which was reported by Verser and Conway in 1960 and 1961, respectively. The measurement of this correlation was being used to test angular correlation equipment built at the US Naval Postgraduate School. Two new experimental determinations of the correlation function with the same equipment as used previously indicated good agreement with the theoretical function. Verser's and Conway's experimentally-determined angular correlation functions were found to deviate less significantly from the theoretical function than they had reported since their standard deviations had failed to take into account the variations of the characteristics of the electronic equipment due solely to electronic causes. It is concluded that the anomaly reported by previous experimenters was statistical in nature.

Programs for the CDC 1604 computer have been developed in FORTRAN language for complete data reduction accepting as input the total counts in each channel, the total coincident counts, and other experimental parameters. The program provides for the calculation of the coefficients for a cosine series and a Legendre polynomial series expansion of the least squares fit to the experimental points. Other programs were developed to calculate the corrections for non-point detectors to be applied to the theoretical coefficients, and to calculate coincidence resolving times from data obtained during a large number of runs.

Major improvements were made in the equipment to be used in future angular correlation experiments, including the construction and testing of both a slow and a fast coincidence unit.

The author wishes to express his appreciation to Associate Professor H. E. Handler who has guided the development of angular correlation measuring equipment at the US Naval Postgraduate School for the last three academic years. His recommendations, particularly in the area of data analysis, and his perusal of the draft of this paper resulted in a still more thorough reinvestigation of the results of the angular correlation studies reported by previous experimenters at this School. It is a pleasure to ackowledge the guidance and aid received from Lt Cmdr P. A. Phelps (USN) in comprehending the theoretical aspects of the basic experiment, in becoming familiar with the electronic equipment, and in writing and debugging the computer programs. Appreciation is expressed to Mr. M. A. Brillhart for his construction of the coincidence units, and for his assistance in developing the mixer circuitry.

TABLE OF CONTENTS

LIST OF FIGURES

LIST OF TABLES

I

INTRODUCTION

A. Purpose of Angular Correlation Experiments

In gamma-gamma angular correlation experiments, one observes the probability of emission of the second quantum of a cascade as a function of angle relative to the first quantum. In general, this probability is an anisotropic function of the angle. Such experiments, in conjunction with other nuclear studies, can lead to identification of the multipole orders of the emissions and the total angular momenta of the original, intermediate, and final states of the nuclide under investigation. [1,2,3] The orientation of the total angular momentum vector of the intermediate level is correlated with the direction of emission of each quantum. The anisotropy of the probability distribution pattern will be attenuated if the orientation of the total angular momentum vector of the intermediate level changes between the times of these two emissions. Thus, one must study a nuclide for which the intermediate energy level has a mean life which is short relative to the period of precession of the angular momentum vector of that level. Only if the total angular momentum vector of the intermediate level does not appreciably change its orientation between the emissions of the two quanta can the probability distribution as a function of angle between the two emissions be interpreted meaningfully.

Generally, no parity assignments can be made for the nuclear levels involved based solely on a directional angular correlation study such as described above, since the angular distribution of the emissions is the same for electric and magnetic multipole radiations of the same order. By means of a similar polarization-direction correlation experiment, wherein one measures the orientation of the polarization vector relative to the plane of the two quanta, one can determine whether the emissions are electric or magnetic multipoles. [4,5] This information, coupled with known multipole orders obtained from an angular correlation study, enables the assignment of relative parities to the three nuclear energy

levels. Absolute parity assignments require additional data.

In the case of Ni^{60}, an even-even nuclide, an even parity and zero total angular momentum are predicted for the ground state on the basis of the nuclear shell model, and are corroborated by other experimental techniques unrelated to this paper. Studies of the decay scheme have shown that the spins of the first and second excited levels are 2 and 4 respectively. Correlation studies are consistent with this and demonstrate that these radiations are pure electric quadrupoles. Thus the complete decay scheme for Ni^{60} is

Decay Scheme of Ni^{60}

Fig. 1

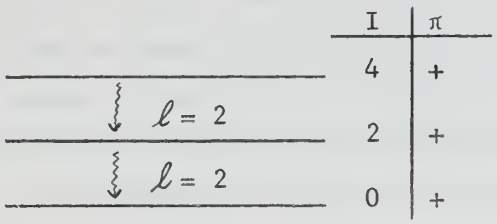

Since this decay scheme is well understood, this gamma-gamma cascade of Ni^{60} is frequently used to determine whether angular correlation equipment is functioning properly. [6] It is used in this manner in this paper.

B. Methods of Conducting the Experiment

Since nuclei are generally randomly oriented, one cannot measure the radiation pattern of a given transition. One way of minimizing the random orientation of the nuclei is to apply a strong magnetic field or a strong electric field gradient at very low temperatures; radiation patterns have been measured using this technique. In the event of a cascade, the effects of this random orientation can be partially circumvented by establishing some reference direction with respect to which only certain of the second of the two radiations are measured. In the experiment discussed in

this paper, nuclei have not been aligned; the reference direction for observation is the direction of emission of the first quantum in the two-gamma cascade of Ni^{60}. Since the lifetime of the intermediate nuclear level for this nuclide is short in comparison with the period of precession of its angular momentum vector, the orientation of the angular momentum vector does not vary significantly between the times of emission of the two quanta. Consequently, an unattenuated angular correlation between the directions of emission of the two successive radiations is observed.

C. Interpretation of the Experimental Data

By measuring the total coincidence counting rate at several angles θ_i between successive quanta, and applying corrections for accidental coincidences and for the attenuation of the correlation function due to the use of detectors of finite size, [7,8] one can determine the relative likelihood of emission of the second quantum at these angles relative to the direction of emission of the first. The experimental estimate of the correlation function at a specific angle θ_i is calculated according to the formula

$$W_{ex}(\theta_i) = \left(\frac{\dot{C}_G}{\dot{N}_1 \dot{N}_2} \right)_i \qquad (1)$$

where $\dot{C}_G$ is the genuine coincidence counting rate at the given angle, and $\dot{N}_1$ and $\dot{N}_2$ are the individual channel counting rates at that angle corrected for the system dead time and background. The least squares fit to these data is the experimental correlation function $W_{ls}(\theta)$. [7] $W_{ls}(\theta)$ is expressed in terms of a linear combination of even powers of cos θ or in terms of a linear combination of even order Legendre polynomials. In the case of the gamma-gamma cascade of Ni^{60}, the theoretical correlation function, $W_{th}(\theta)$, corrected for the solid angles subtended by the detectors used in this experiment is given by

$$W_{th}(\theta) = 1.00000 + 0.09960\ P_2(\cos\theta) + 0.00838\ P_4(\cos\theta) \quad . \qquad (2)$$

Experimental results can be compared with theory by comparing the coefficients calculated in the least squares fit with the above coefficients. In addition, one can compare the experimentally-determined anisotropy with the theoretical value. The anisotropy is defined as follows:

$$R = \frac{W_{ls}(180^{o})}{W_{ls}(90^{o})} - 1 \ . \qquad (3)$$

The theoretical value of R, corrected for the geometry of this experiment is + 0.16221. A close agreement between the experimental and theoretical coefficients and between the experimental and theoretical anisotropies provides a check of proper equipment operation.

D. Previous Work in This Field at U.S. Naval Postgraduate School

The basic equipment for this experiment was assembled in academic year 1959-60 by Verser [9], who conducted an angular correlation experiment in the 90-180° quadrant and reported agreement with the theoretical anisotropy but reported marked deviation from theory in the shape of the experimental curve. The equipment was modified slightly in academic year 1960-61 by Conway [10] who performed the same experiment in the same quadrant and also reported a similar deviation from theory in the shape of the experimental curve. Fig (2) shows the results of these investigations. Verser reported a dip in his experimental curve which deviated by more than two standard deviations from the theoretical curve in the 120-135° region. Conway reported a similar dip in the vicinity of 135°, and a less pronounced dip in the 120° region.

Conway wrote two programs in CDC 1604 computer assembly routine language, one for the least squares fit of a linear combination of Legendre polynomials of even order to the experimental data, and a second to calculate the solid angle corrections necessitated by the finite size of the detectors. The least squares program required a considerable amount of hand-calculated data reduction before it could be used.

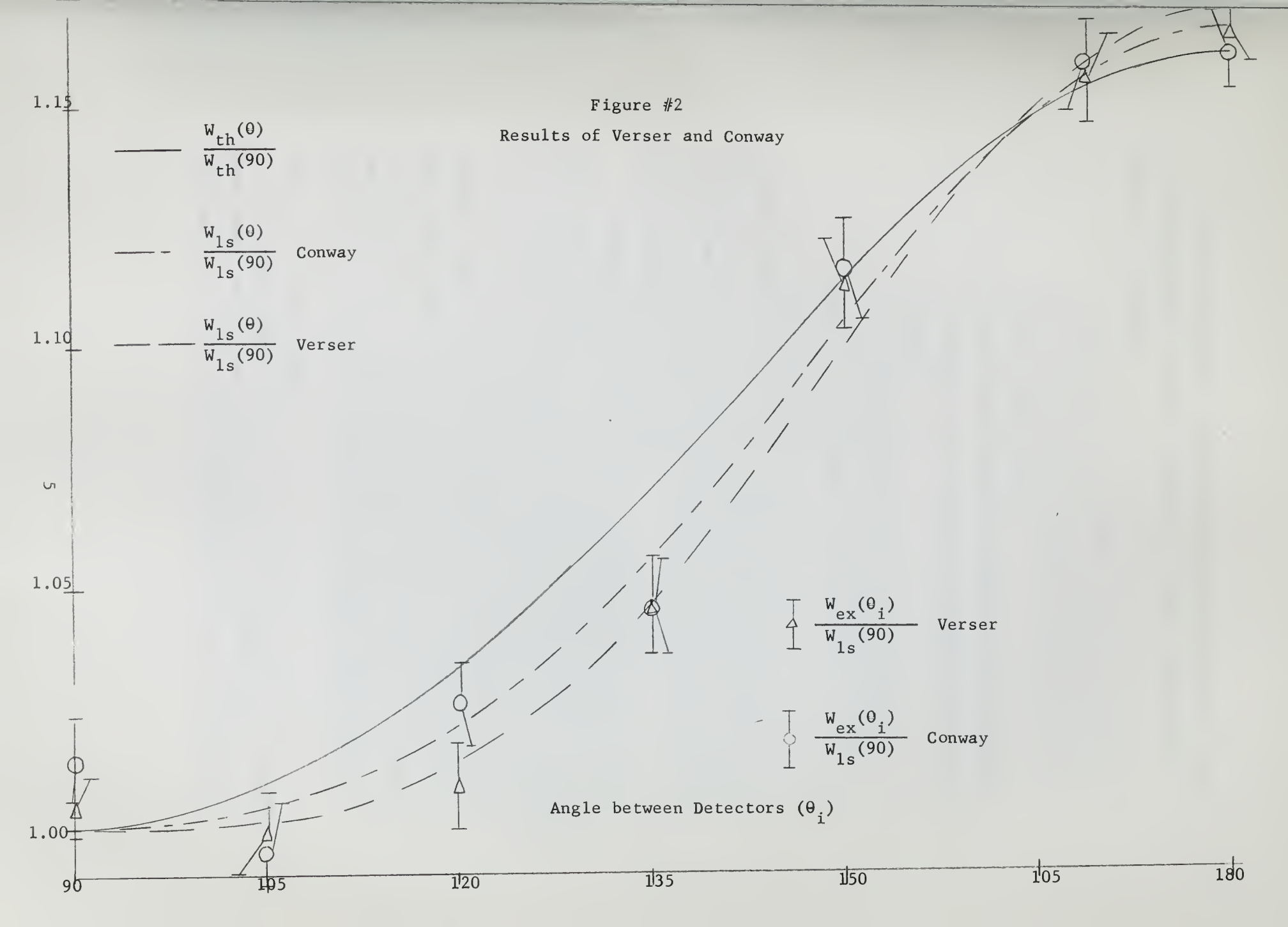
Figure #2
Results of Verser and Conway
$\frac{W_{th}(\theta)}{W_{th}(90)}$
$\frac{W_{ls}(\theta)}{W_{ls}(90)}$ Conway
$\frac{W_{ls}(\theta)}{W_{ls}(90)}$ Verser
$\frac{W_{ex}(\theta_i)}{W_{ls}(90)}$ Verser
$\frac{W_{ex}(\theta_i)}{W_{ls}(90)}$ Conway
1.15
1.10
1.05
1.00
90
105
120
135
150
105
180
Angle between Detectors (θ_i)

Possible mechanisms underlying the reported anomalous dip in the experimental curve as suggested by Verser and Conway include the following:

1. A change in the condition of the source, possibly crystallization resulting in preferential alignment of the nuclei within the crystal due to internal electric fields.
2. Fluctuations of ambient temperature which resulted in changes in the operating characteristics of the equipment.
3. Uncompensated variations in line voltage.
4. Perturbing effects of external magnetic fields.
5. Improper orientation of the source relative to the detectors.

It was recognized that the likelihood of having any noticeable effects due to Items "1" or "4" above at room temperature was extremely small since the Boltzmann factor for the relative populations of the energy levels is nearly unity except under the influence of extremely strong fields.

In addition, the possibility was recognized of there being in fact no real anomaly, but that the discrepancy was simply an unlikely statistical occurrence or that some systematic error existed in the experimental technique, in the processing of data by hand, or in one of the previous computer programs. The likelihood of this deviation from the theoretical being simply a statistical fluke became greater when it was recognized that the variation in the resolving time of the coincidence unit was not taken into account in computation of the standard deviation of the correlation function evaluated at the angles at which the experiments were conducted.

E. Scope of the Investigation

Many experimenters have reported agreement with the theoretical gamma-gamma angular correlation function for Ni^{60} [11,12], yet two experimenters at this School independently reported a significant

deviation from theory in the 105-135° region. Thus it was clear that before one could use this equipment for the experiments for which it was assembled; namely, experiments with short-lived nuclides, further investigation was necessary either to arrive at a mechanism for the reported anomaly, or to demonstrate that the anomaly, under more closely controlled experimental conditions, is not observed. In the investigation of this anomaly, certain improvements were made in the experimental equipment; new programs in FORTRAN language were developed to compute the solid angle corrections to the angular correlation function and calculate the least squares fit; and experiments were conducted under closely controlled conditions in both the 90-180° and the 180-270° quadrants to see whether a similar dip would be observed.

Two additional coincidence units were constructed. One of these is a slow coincidence unit which, unlike that used by Verser and Conway, has a resolving time which is independent of counting rate. This characteristic will be required in conjunction with future experiments with short-lived nuclides. The second coincidence unit has a resolving time an order of magnitude shorter than that of the slow units. The use of the fast unit in conjunction with a slow unit enables one to achieve better precision by reducing the accidental coincidence counting rate.

II

REINVESTIGATION OF THE EARLIER REPORTED ANOMALY

A. Equipment Used

The experimental setup employed by Verser and Conway is described in detail elsewhere [9,10]. Figure (3) indicates the general test setup and Figure (4) shows the angular correlation table with the source, crystals, photomultiplier tubes, and preamplifiers. The same slow coincidence unit as used by Verser and Conway was used in the angular correlation experiments in the 90-180° and in the 180-270° quadrants. The only significant change in the setup for these experiments consisted of adding a voltage regulator to minimize the effects of uncompensated line voltage fluctuations. Regulated voltage was then supplied to those parts of the electronic apparatus most likely to distort the experimental measurements when under the influence of line voltage fluctuations. These included the coincidence unit, both linear amplifiers, and the high voltage power supply for the photomultiplier tubes.

B. Coincidence Resolving Time Tests

The accidental coincidence counting rate is calculated from the usual formula

$$\dot{C}_A = 2\tau \dot{N}_1 \dot{N}_2, \qquad (4)$$

where τ is the coincidence resolving time. Before and during the angular correlation experiments, scores of tests were conducted to determine the stability and the magnitude of τ. The unit exhibited random fluctuations in resolving time as much as three times as large as those that can be explained in terms of nuclear statistics. The fractional variation in τ, $\frac{\sigma(\tau)}{\tau}$ was observed to be approximately twice that reported by Verser and Conway. The measured mean is 0.2470 microseconds. The variance of a single measurement of τ is 0.0044 microseconds; this includes the variation due to non-nuclear fluctuations and was used in calculating the variance of the accidental coincidence counting rates in this work. Since the resolving-

Figure 3. Experimental Setup of Verser and Conway

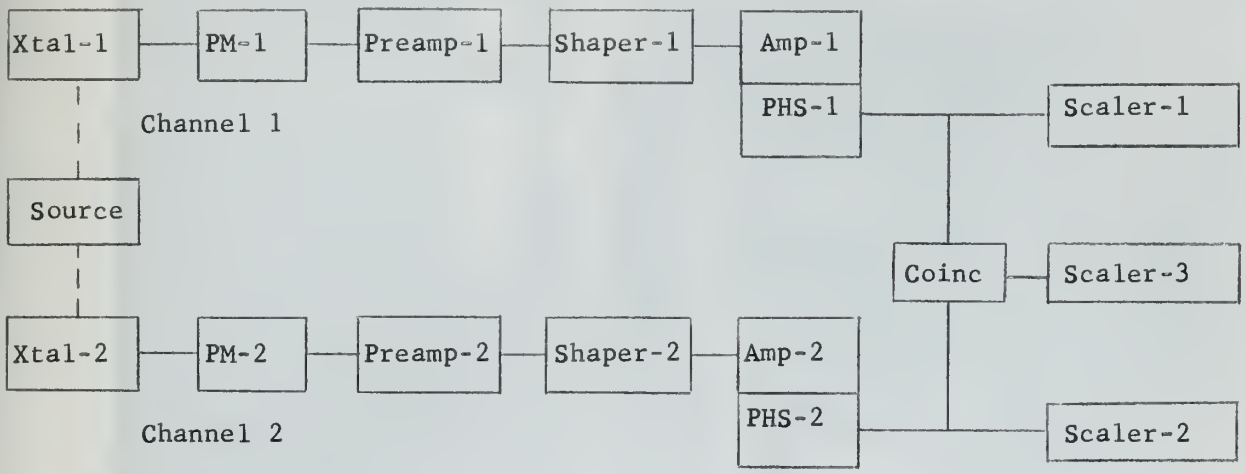

Xtal's = Harshaw Scintillator Crystals, Type 8S8/2.(2" diam x2" thick)

PM's = RCA 6342 Photomultipler Tubes
Power for PM tubes from Hamner H.V. Power Supply Model N-401

Amp's = Hamner N302 Amplifiers - each includes a differential pulse height analyzer which supplies a standard pulse out ("PHS" out) (A linearly amplified input is also supplied as an output but was not used in this experimental setup).

Coinc = Coincidence Analyzer, Atomic Model 502A.

Scalers = Baird-Atomic, Model 1283

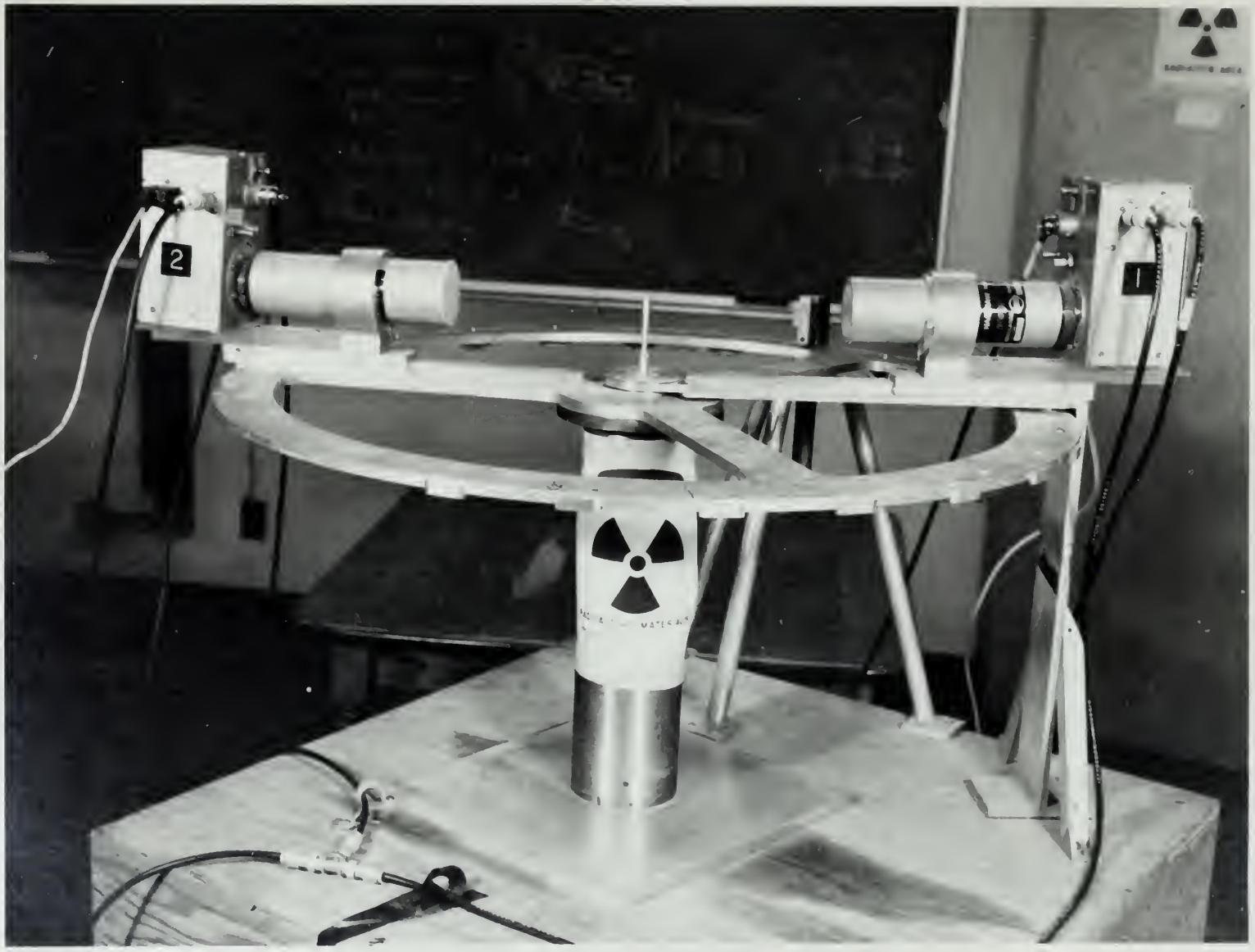

Fig. 4 Angular Correlation Table

time characteristics were investigated and documented far more completely than in previous years, the observed instability was felt to be similar to that which would have been found by the earlier experimenters had they investigated this problem more thoroughly. An inclusion of the effect of this fluctuation in the analysis of their data would decrease their reported precision.

C. Daily Checkout Procedure and Instrument Log

A daily checkout procedure was devised to ensure that exactly the same checks of the operating characteristics of the electronic equipment were performed each day in the same sequence and with the equipment in the same operating configuration at each stage of the checkout.

An instrument log was developed in which the experimental equipment layout was recorded, and monitoring points for key wave shapes were indicated. Photographs of these key wave shapes are included, as well as the record of the oscilloscope settings used when the photographs were taken; a sample page from this log is shown in Figure 5 . This log has proven useful in trouble-shooting the extensive circuitry and for monitoring changes in operating characteristics, such as pulse rise times, which could degrade system performance.

D. Scaler Dead Time

As a part of the complete checkout and alignment of all electronic gear prior to conducting the angular correlation experiments, two-source experiments were run to determine the system resolving time (primarily scaler dead time). Several of these measurements all led to the same surprising result, namely, a negative dead time for the system. Further investigation of this problem involved supplying pairs of pulses from a double pulse generator at a constant repetition rate and varying the time between the pulses of each pair. Expected behavior was that with the 1000 per second repetition rate for the pair of pulses, 2000 counts per second would be registered on the scalers as long as the separation between the pulses of each pair exceeded the

Monitor Point 15

	v/cm	μs/cm	probe	exp
top	2.5	0.1	yes	3
middle	2.5	0.1	yes	2
bottom	2.5	0.5	yes	2

Monitor Point 22

	v/cm	μs/cm	probe	exp
top	0.5	0.1	no	4
middle	0.5	0.1	no	3
bottom	0.5	1.0	no	2

Monitor Point 23

	v/cm	μs/cm	probe	exp
top	10.0	0.1	yes	3
middle	10.0	0.1	yes	2
bottom	10.0	0.5	yes	2

Monitor Point 24

	v/cm	μs/cm	probe	exp
top	10.0	0.1	yes	2
middle	10.0	0.1	yes	3
bottom	10.0	0.5	yes	2

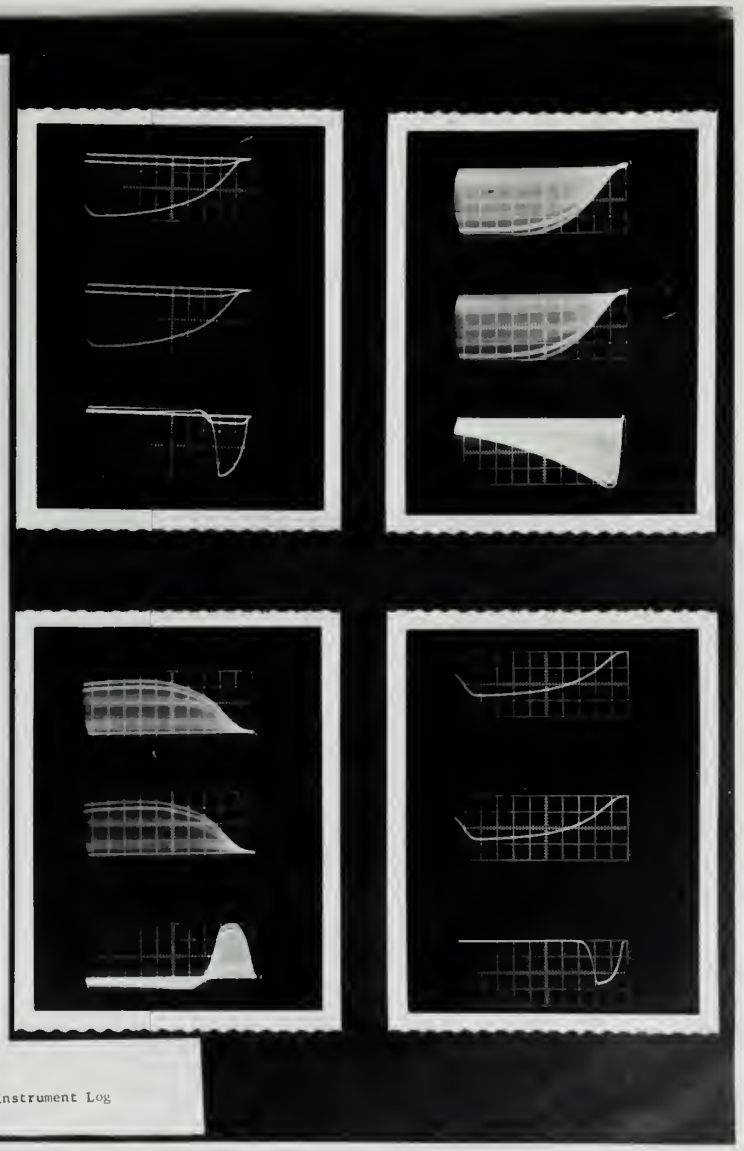

Fig. 5. Instrument Log

resolving time of the system. When the separation between the two pulses was less than the resolving time of the system, 1000 counts per second would be expected. What was observed was the recording of 2000 counts per second when the interval between the pulses of each pair was greater than about 5-10 microseconds, then as the interval was decreased, the count rate recorded by the scalers increased, on occasion by as much as 25%; i.e., to about 2500 counts per second.

Since the experimentally-determined correlation function is not sensitive to the introduction of these spurious counts because the error introduced into the single channel counting rates is essentially constant for all angles and the effect on the coincidence counting rate is negligible, this anomalous behavior had no significant influence on the experimental results reported herein. New scalers will be employed for future experiments.

E. Calculation of the Standard Deviation of $W_{ex}(\theta_i)$

The method of calculating the standard deviation of the experimental estimate of the correlation function has been the subject of extensive consideration. The experimental estimate of the correlation function at a specific angle θ_i is calculated according to the formula

$$W_{ex}(\theta_i) = \left(\frac{\dot{C}_G}{\dot{N}_1 \dot{N}_2} \right)_i \qquad (1)$$

where $\dot{C}_G$ is the genuine coincidence counting rate at the given angle, and $\dot{N}_1$ and $\dot{N}_2$ are the individual channel counting rates at that angle corrected for the system dead time and background. The genuine coincidence counting rate is calculated from

$$\dot{C}_G = \dot{C}_T - \dot{C}_A, \qquad (5)$$

where $\dot{C}_G$ = the genuine coincidence counting rate, $\dot{C}_T$ = the total coincidence counting rate, and $\dot{C}_A$ = the accidental coincidence counting rate.

$\dot{C}_T$ and the single channel counts were measured directly by scalers and the accidental coincidence rate was calculated from

$$\dot{C}_A = 2\tau \dot{N}_1 \dot{N}_2 . \tag{6}$$

It can be seen that the standard deviation of $W_{ex}(\theta_i)$ depends almost entirely upon that of $\dot{C}_G$. The standard deviation of $\dot{C}_G$ is obtained by taking the square root of the sum of the variances of the two presumably independent quantities, $\dot{C}_T$ and $\dot{C}_A$

$$\sigma(\dot{C}_G) = \sqrt{\sigma^2(\dot{C}_T) + \sigma^2(\dot{C}_A)} \tag{7}$$

Verser and Conway calculated this standard deviation assuming that the distributions of $\dot{C}_A$ and $\dot{C}_T$ are Poisson in nature and therefore that the variances are expressible as:

$$\sigma^2(\dot{C}_A) = \frac{\dot{C}_A}{t} \quad \text{and} \quad \sigma^2(\dot{C}_T) = \frac{\dot{C}_T}{t} \tag{8a,b}$$

where t is the duration of the measurement. Therefore they calculated $\sigma(\dot{C}_G)$ from the relation

$$\sigma(\dot{C}_G) = \sqrt{\frac{\dot{C}_T}{t} + \frac{\dot{C}_A}{t}} . \tag{9}$$

If the equipment used in the experiment were perfectly stable, with no changes in τ due to changes in electronic characteristics, then all fluctuations in $\dot{C}_A$ and $\dot{C}_G$ would be consistent with Poisson distributions and these equations would apply. As pointed out in Section B, $\sigma^2(\dot{C}_A)$ when calculated from equation 8a is too small. To calculate a realistic variance of $\dot{C}_A$, one must provide not only for the statistical variations due to the random nature of the radioactive decay process, but also for the variations in the resolving time of the coincidence unit due to changes in its electronic operating characteristics.

If electronic instabilities were present and nuclear fluctuations were small in comparison thereto, then the variance of $\dot{C}_A$ would be described adequately by the relation

$$\sigma^2_{elec}(\dot{C}_A) = \left[\sigma^2_{elec}(\tau)\right]\left[2\dot{N}_1\dot{N}_2\right]^2$$

$$= \left[\frac{\sigma_{elec}(\tau)}{\tau}\right]^2 \dot{C}_A^{\,2}, \text{ by equation (6)}$$

$$\text{Then } \sigma^2_{elec}(\dot{C}_A) = \left[\frac{\sigma_{elec}(\tau)}{\tau}\right]^2 \dot{C}_A^{\,2} \qquad (10)$$

where σ_{elec} denotes the standard deviation due solely to the electronic instability of the coincidence unit.

Since under experimental conditionsneither of the two limiting conditions obtains; i.e., perfect equipment stability in which case the variance of $\dot{C}_A$ would be Poisson, or infinite counting time in which case nuclear fluctuations would be insignificant in comparison with $\sigma_{elec}(\dot{C}_A)$, both statistical deviations must be taken into account in calculating $\sigma^2(\dot{C}_A)$. While the technique for the rigorous statistical combination of these variances is not certain in spite of efforts to arrive at a valid analytical expression, the rather naive approach of adding them would seem to be a conservative approach which applies to the experimental situation. Thus the expression used in this report for calculating $\sigma^2(\dot{C}_G)$ is:

$$\sigma^2(\dot{C}_G) = \frac{\dot{C}_T}{t} + \frac{\dot{C}_A}{t} + \left[\frac{\sigma_{elec}(\tau)}{\tau}\right]^2 \dot{C}_A^{\,2} \qquad (11)$$

It can be seen that this expression gives the correct standard deviation in the two limiting cases discussed earlier, and it is assumed that the error resulting from applying this expression in the actual situation is small.

On the basis of the experimental determination of τ, the third term of this expression is of the same order as the first two; hence, failing to take it into account results in unrealistically small estimates of the uncertainties in the experiment.

F. Preparation and Check of New Computer Programs

Conway prepared two programs in 1960-61 in 1604 computer assembly routine language. The purpose of one was to calculate the solid angle correction following the scheme of Rose [8] to apply to the theoretical correlation function to account for the attenuation resulting from the finite dimensions of the detectors. The second program calculated the coefficients for a least squares fit [7] of even order Legendre polynomials to $W_{ex}(\theta_i)$.

As mentioned previously, difficulties were experienced in attempting to run these programs. In addition, the least squares program required the following prior manual computations:

1. application of scaler dead time corrections
2. correction of counting rates for background
3. calculation of $\dot{C}_A$ and $\sigma^2(\dot{C}_A)$
4. calculation of $\dot{C}_G$ and $\sigma^2(\dot{C}_G)$
5. calculation of $W_{ex}(\theta_i)$ and $\sigma^2\left[W_{ex}(\theta_i)\right]$
6. calculation of a weighted mean of $W_{ex}(\theta_i)$ at each angle
7. calculation of the standard deviation of the weighted mean at each angle

The values of the weighted mean of $W_{ex}(\theta_i)$ and the standard deviation of the weighted mean at each angle were the entering arguments for Conway's least squares program.

The original intent was to program the above listed preliminary computations only, and to append Conway's least squares program as a subroutine. It was not possible to append his program to the FORTRAN program, however, due to the incompatibility of the two computer languages. A FORTRAN program was written to accept as input the total

counts registered by the scalers and thus save considerable time and achieve greater accuracy by avoiding the errors likely to creep into the lengthy manual computations.

Separate programs were written which would compute the coefficients for the even power cosine series as well as the coefficients for the even order Legendre polynomial series representation of $W_{ls}(\theta)$, calculate the solid angle corrections to be applied to $W_{th}(\theta)$, and calculate τ from the data obtained during coincidence resolving time runs.

The above programs provided independent checks of Conway's least squares and solid angle correction programs. The new least squares program proved extremely useful during the reanalysis of earlier data as it permitted repeated reduction of the same experimental data with incrementally varied input parameters.

The FORTRAN programs together with a glossary of terms is included in the Appendix(A thru E.)

To check the operation of the FORTRAN programs, they were used to perform the same least squares and solid angle correction computations as performed earlier by Verser and Conway, and the results compared with their earlier results, as follows.

1. The same geometrical parameters as used by Verser and Conway were used as the entering arguments for the FORTRAN solid angle correction program. Good agreement was reached with Verser's hand-calculated values and Conway's computed values.
2. The raw data (scaler counts) or Verser were used as the entering arguments for the FORTRAN least squares program. Good agreement was reached with Verser's values of the mean values of $W_{ex}(\theta_i)$, and with his coefficients for the Legendre series representation of $W_{ls}(\theta)$ thus indicating proper operation of the preliminary and subsequent portions of this program.

3. The results of analysis of Conway's data with the FORTRAN program did not agree with the results of analysis which he reported. Some significant arithmetical errors were uncovered in the hand calculations which he was required to perform prior to entering his program. When these errors were corrected, agreement was realized in the results of analysis by the two programs, providing another check of the FORTRAN least squares program.

G. Reanalysis of Earlier Data

Once assured that the new FORTRAN programs were operating properly, Verser's data and a portion of Conway's data were reanalyzed, including in the calculation of the variances the effect of the electronic instability of the coincidence unit.

In checking over the data collected by Conway, it was noted that they were collected during two relatively short periods of time spaced nearly four months apart. During these four months a significant change in the strength of the Co^{60} source ($T_{1/2} \sim 5.2$ years) occurred; this had not been corrected for in his data analysis. The reanalysis of his experiment was done using only his later set of data.

It became apparent that the scatter of Conway's data about $W_{ls}(\theta)$ was greater than the standard deviations would imply. Consequently, estimates of the values of $\sigma\left[W_{ex}(\theta_i)\right]$ were calculated based upon the actual residuals between the experimental points and $W_{ls}(\theta)$ for his later set of data. This calculation, which took into account the electronic variations of the equipment, resulted in values for

$$\frac{\sigma\left[W_{ex}(\theta_i)\right]}{W_{ex}(\theta_i)}$$

approximately three times as large as the values which Conway quoted.

The results of the reanalysis of the previous data are tabulated below and are presented graphically in Figure 6a and 6b. It is evident that the anomaly in the 120-135^{o} region still exists in Verser's results, though it is not as significant statistically as previously reported due to the larger standard deviations. The analysis of Conway's data now shows no evidence of a dip.

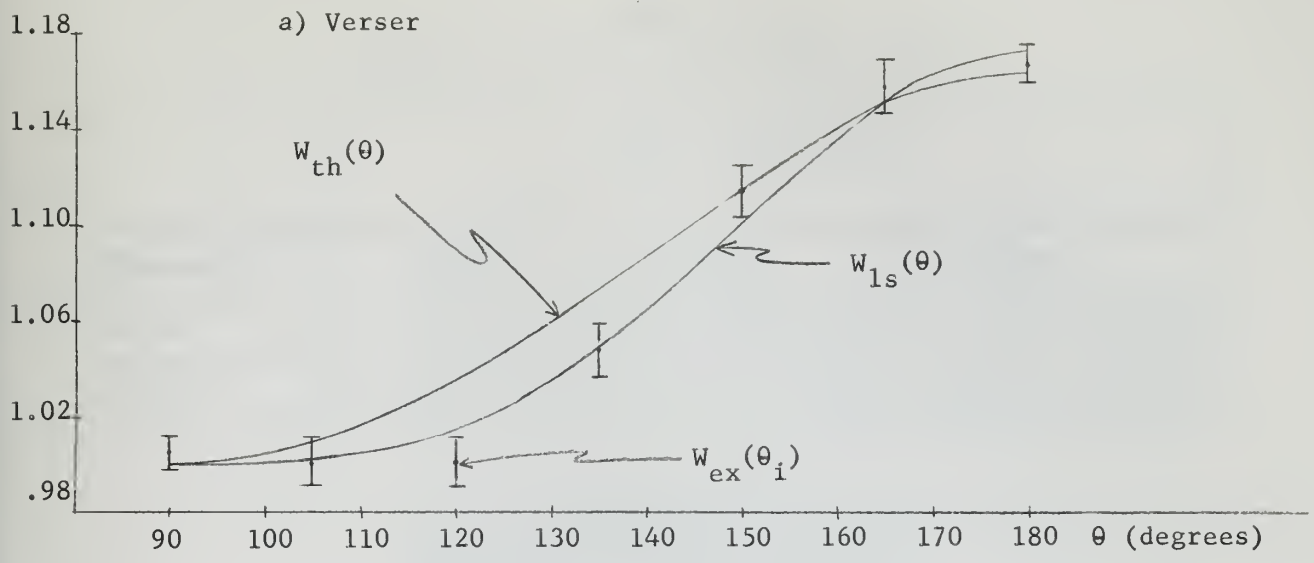

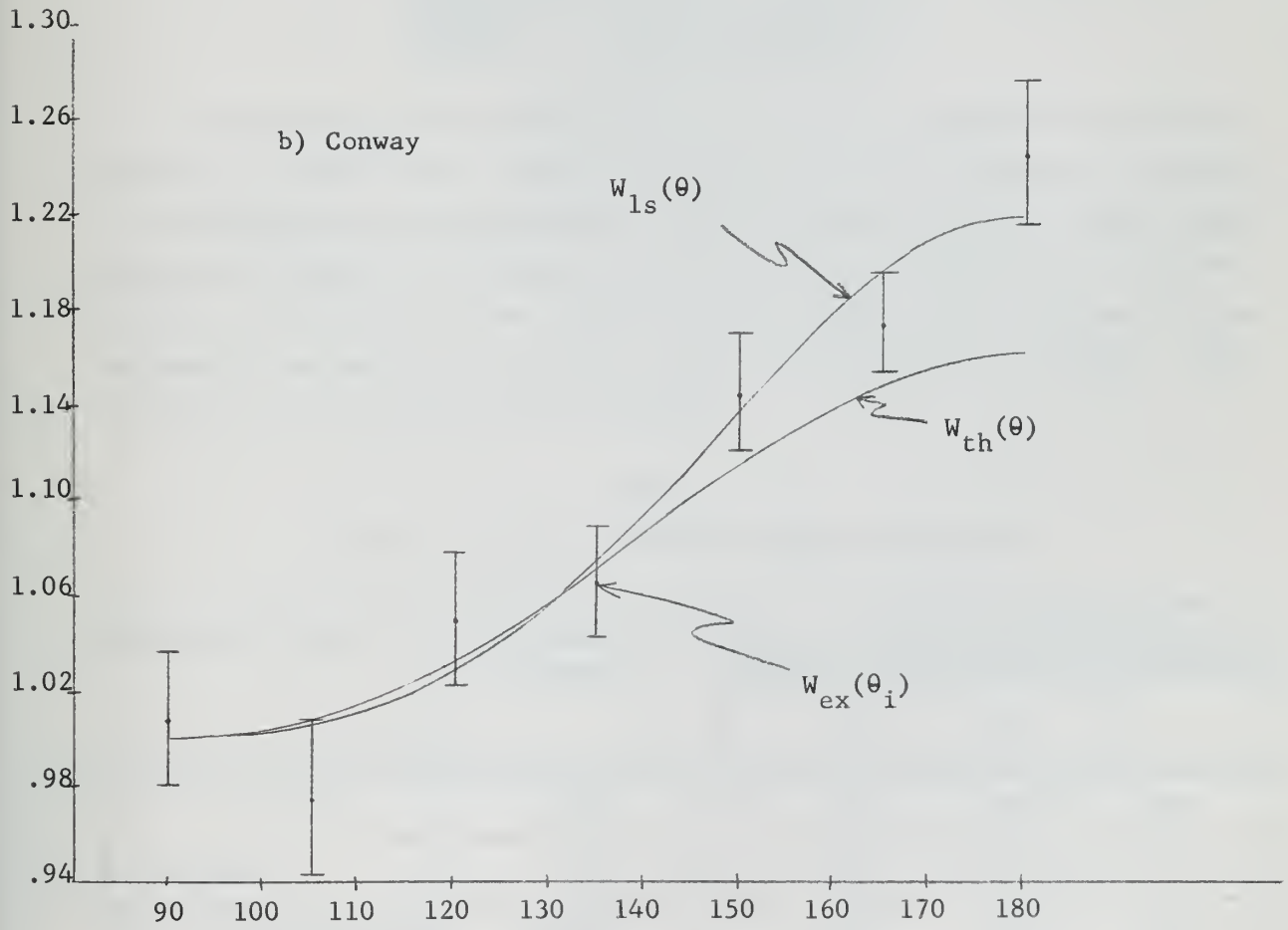

Reanalysis of Data of Verser and Conway

Fig. 6a, b

Table 1

Results of Reanalysis of Earlier Data

	Legendre Coefficients			Anisotropy
	a_o	a_2	a_4	
Theoretical	1.0000	0.0996	0.0084	0.162
Verser	1.0000 $\pm$ 0.0042	0.0960 $\pm$ 0.0068	0.0337 $\pm$ 0.0087	0.171 $\pm$ 0.026
Conway	1.000 $\pm$ 0.011	0.126 $\pm$ 0.020	0.032 $\pm$ 0.023	0.220 $\pm$ 0.079

The possibility was investigated that errors could have been introduced into Verser's data analysis through the use of incorrect parameters. In investigating this possibility, raw data gathered by both Verser and Conway were used as the entering arguments for the FORTRAN least squares program, and these data were reduced while systematically varying the experimental parameters to see what effect this would have on $W_{1s}(\theta)$. The results of this analysis are as follows:

Table 2

Effect on $W_{1s}(\theta)$ of Varying Input Parameters

Parameter Varied	% Variation in Parameter	Resulting % Variation		
		Legendre Coefficients		Anisotropy
		a_2	a_4	
τ	$\pm$ 10%	$\pm$8%	$\pm$8%	$\pm$8%
Background	+ 6%	0%	0%	0%
Scaler Resolving Time	+500%	+3%	+3%	+5%

It can be seen from the above that the shape of $W_{1s}(\theta)$ is relatively insensitive to changes in background and changes in the resolving time

of the scalers. However the shape of $W_{1s}(\theta)$ varies appreciably when τ varies. The reason for these changes in $W_{1s}(\theta)$ is clear from the following. If the numerical value used for τ is greater than the actual τ of the coincidence unit during the experiment, then too many accidental coincidences are subtracted from the total coincidences in calculating the number of genuine coincidences. Thus the apparent value of $\dot{C}_G$ is smaller than was actually realized experimentally. Since the error introduced into $\dot{C}_A$ is constant at all angles, assuming that $\dot{N}_1$ and $\dot{N}_2$ are independent of θ, which is approximately true, the error introduced into $\dot{C}_G$ is also constant at all angles. Since in these experiments, the ratio of the accidental coincidence counting rate to the genuine coincidence counting rate is about 2:3 and it can be seen from the expression

$$R_{th} = \left(\frac{W_{1s}(180)}{W_{1s}(90)} \right) - 1 = .167 \qquad (3)$$

that $W_{1s}(90)$ is more sensitive than $W_{1s}(180)$ to changes in the genuine coincidence counting rate, it is apparent that the calculated anisotropy increases when the coincidence resolving time is increased. It is stressed that the shape of $W_{1s}(\theta)$ is distorted by using a value of τ in the data reduction which does not correspond to the value of τ actually characteristic of the coincidence unit during the experiment. The shape of $W_{1s}(\theta)$ is independent of τ as long as the true experimental value of τ is used in calculating $\dot{C}_A$.

The effect upon the shape of $W_{1s}(\theta)$ of using incorrect parameters for the geometry of the experiment was investigated also, by progressively varying the entering arguments for the FORTRAN solid angle correction program. The results of this analysis are given in in Table 3.

Table 3

Effect on Solid Angle Corrections of Varying Input Parameters

Parameter Varied	Amount Varied	Relative Change in Absorption Coefficients	
		Q_2	Q_4
Linear absorption coefficient of the crystal	± 10%	0.00%	0.00%
Distance from source to crystal	± 8.5%	0.00%	0.00%
Crystal radius	± 1.0%	0.00%	0.00%
Crystal thickness	± 1.0%	0.00%	0.00%

It can be seen that the shape of $W_{ls}(\theta)$ is relatively insensitive to changes in these geometrical parameters over the range investigated.

It is concluded from these investigations of the effects upon the least squares analysis and solid angle correction computations of varying the entering arguments, that none of these can account for the dip reported by Verser.

H. Analysis of New Data

The results of the analysis of the data obtained with the old slow coincidence unit in experiments in two separate quadrants are indicated graphically in Fig. 7. When the data from each of these two experiments were reduced separately, $W_{ls}(\theta)$ agreed with $W_{th}(\theta)$ within the statistical error of the experiment. Since the angular correlation function is symmetrical about 180^{o}, it was possible to combine the results of the analysis of the data obtained during the experiment in the 90 - 180^{o} quadrant with those obtained during the the experiment in the 180 - 270^{o} quadrant. The purpose of combining the results in this way was to benefit from the decrease in $\sigma\left[W_{ex}(\theta_i)\right]$ resulting from the analysis of a greater quantity of data, thus being able to compare more precisely $W_{ls}(\theta)$ and $W_{th}(\theta)$.

Due to the time interval between the two experiments, during which the source decayed significantly, the raw data from the two experiments cannot be combined. Consequently, the data obtained from each experiment were analyzed independently, then the normalized values of the weighted mean of $W_{ex}(\theta_i)$ from the two experiments were combined using as weighting factors the reciprocals of their variances. These composite values of $W_{ex}(\theta_i)$ were then used as the entering arguments for the least squares subroutine to generate a new $W_{ls}(\theta)$.

The results of the new experiments are tabulated below.

Table 4
Results of Analysis of New Data

	Experimental			Theoretical
	Quadrant		Composite	
	180^{o}-270^{o}	90-180^{o}		
Anisotropy	0.151 ± 0.029	0.165 ± 0.034	0.158 ± 0.018	0.162
Legendre Coefficients				
a_o	1.0000 ± 0.0057	1.0000 ± 0.0057	1.0000 ± 0.0040	1.0000
a_2	0.092 ± 0.010	0.1062 ± 0.0094	0.0987 ± 0.0069	0.0996
a_4	0.010 ± 0.012	-0.005 ± 0.012	0.0036 ± 0.0085	0.0084

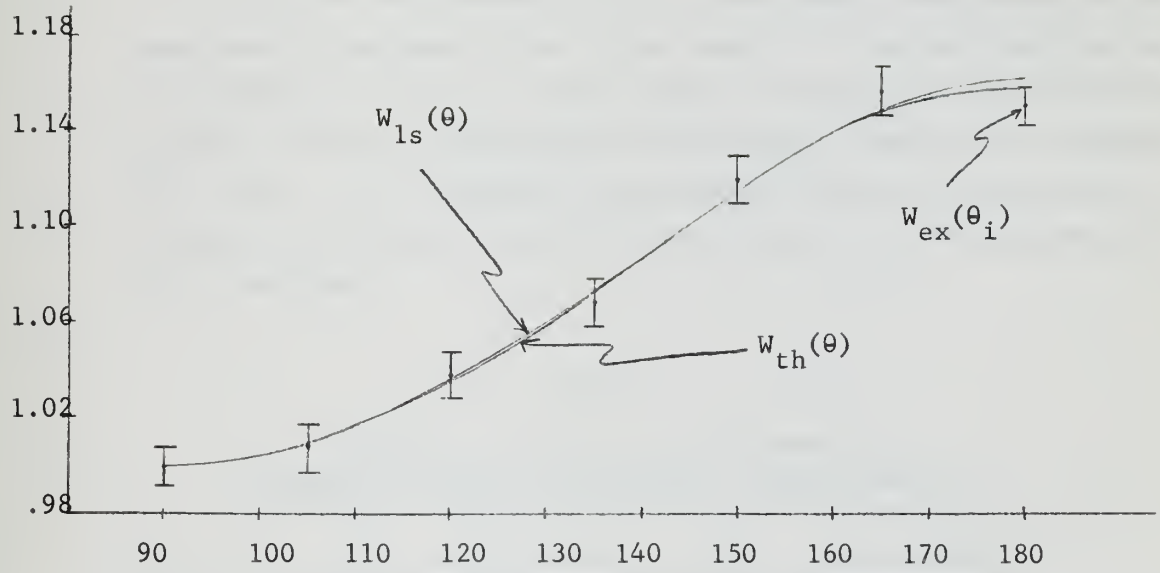

Results of Analysis of New Data

Fig. 7.

I. Comparison of Experimental Results with Theory

All of Verser's data, and the portion of Conway's data used in the reanalysis of his data (see Section G) were combined with the data obtained during the two new experiments according to the scheme discussed in the previous section. That is, the data from each of the four experiments were analyzed independently, then the weighted means of the normalized mean values of $W_{ex}(\theta_i)$ from the four experiments were used as the entering arguments for the least squares subroutine. The results of this combination of these data are indicated graphically in fig. 8, and are tabulated in Table 5. No significant deviation from $W_{th}(\theta)$ is evident.

While the real demonstration of the proper functioning of the experimental equipment lies in the results of the new experiments in two quadrants, it is of interest that no significant deviation from $W_{th}(\theta)$ occurs even when Verser's and Conway's results are combined with these. It is concluded that the dip which they reported is strictly a statistical fluke and that there is no actual physical effect involved.

Table 5

Results of Composite Data Analysis
(Composite Results based upon 4 experiments)

	Experimental	Theoretical
Anisotropy	0.169 ± 0.018	0.162
Legendre Coefficients		
a_o	1.0000 ± 0.0028	1.0000
a_2	0.1000 ± 0.0047	0.0996
a_4	0.0183 ± 0.0058	0.0084

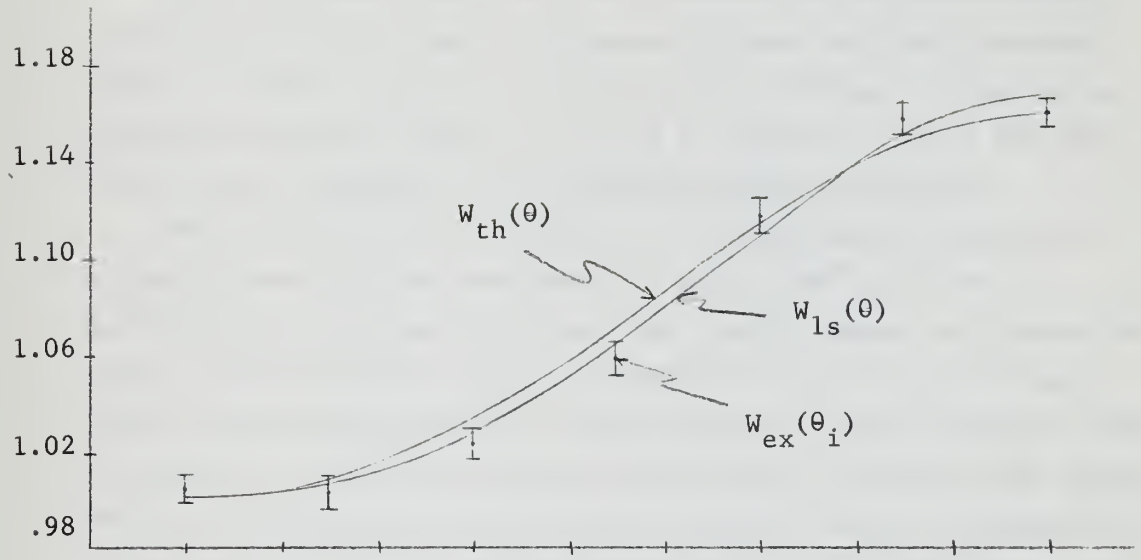

Results of Composite Data Analysis

Fig. 8.

III

DEVELOPMENT OF NEW INSTRUMENTATION

A. New Slow Coincidence Unit

While investigating the earlier reported anomaly in $W_{ls}(\theta)$ in the 105-135° region, work proceeded on building and testing a new slow coincidence unit incorporating certain portions of the design reported by Garg [13]. This design features a variable resolving time which is independent of the counting rate. The slow coincidence unit used by Verser and Conway lacked both of these features.

The coincidence unit which was constructed differed markedly from Garg's only in that the separate channel amplitude discriminators of Garg's unit were deleted since differential discrimination was performed earlier (Fig. 9). Figure 10 gives the complete circuit diagram for the unit which was constructed.

The new slow unit was tested by incorporating it into the circuitry used for the experiment in the 90-180° quadrant in parallel with the slow coincidence unit which Verser and Conway had used. The correlation function measured by the two slow coincidence units agreed within the uncertainties in their resolving times. The results of numerous resolving time tests of the new slow coincidence unit indicated a greater long time drift than is characteristic of the old slow unit. This increased drift of τ necessitates more frequent determinations of its magnitude and required using different values for τ during the angular correlation runs, rather than using a mean value of τ based upon a large number of resolving time runs such as was done with the old slow coincidence unit.

B. Requirement for a Fast Coincidence Unit

1. General

A coincidence unit of significantly shorter resolving time than that of the unit used by Verser and Conway was required to improve the statistical error in the experimental estimate of the correlation function, $W_{ex}(\theta_i)$. Better statistics were required for the reinvestigation of the earlier reported anomaly

Figure 9. Block Diagram, New Slow Coincidence Unit

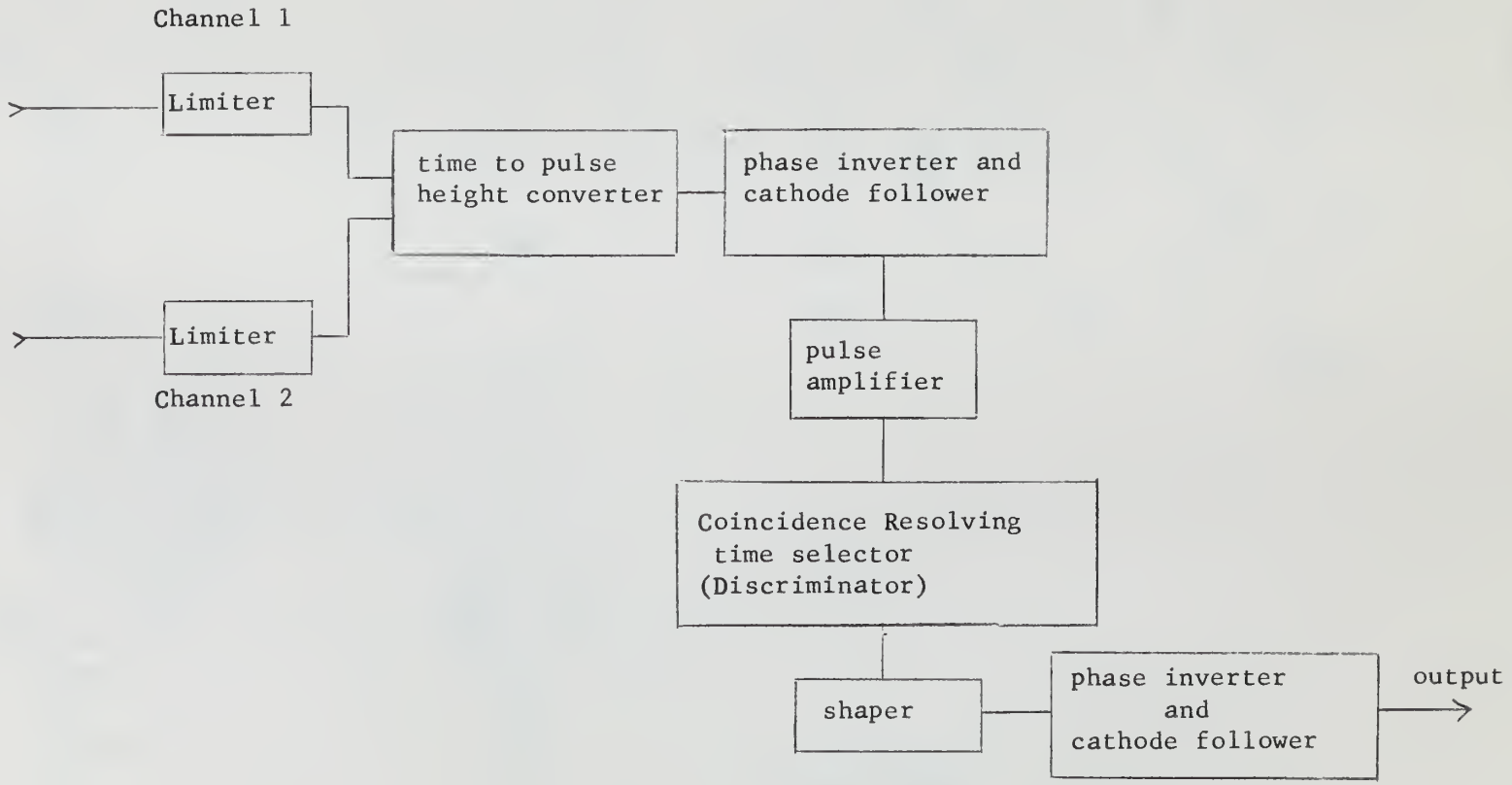

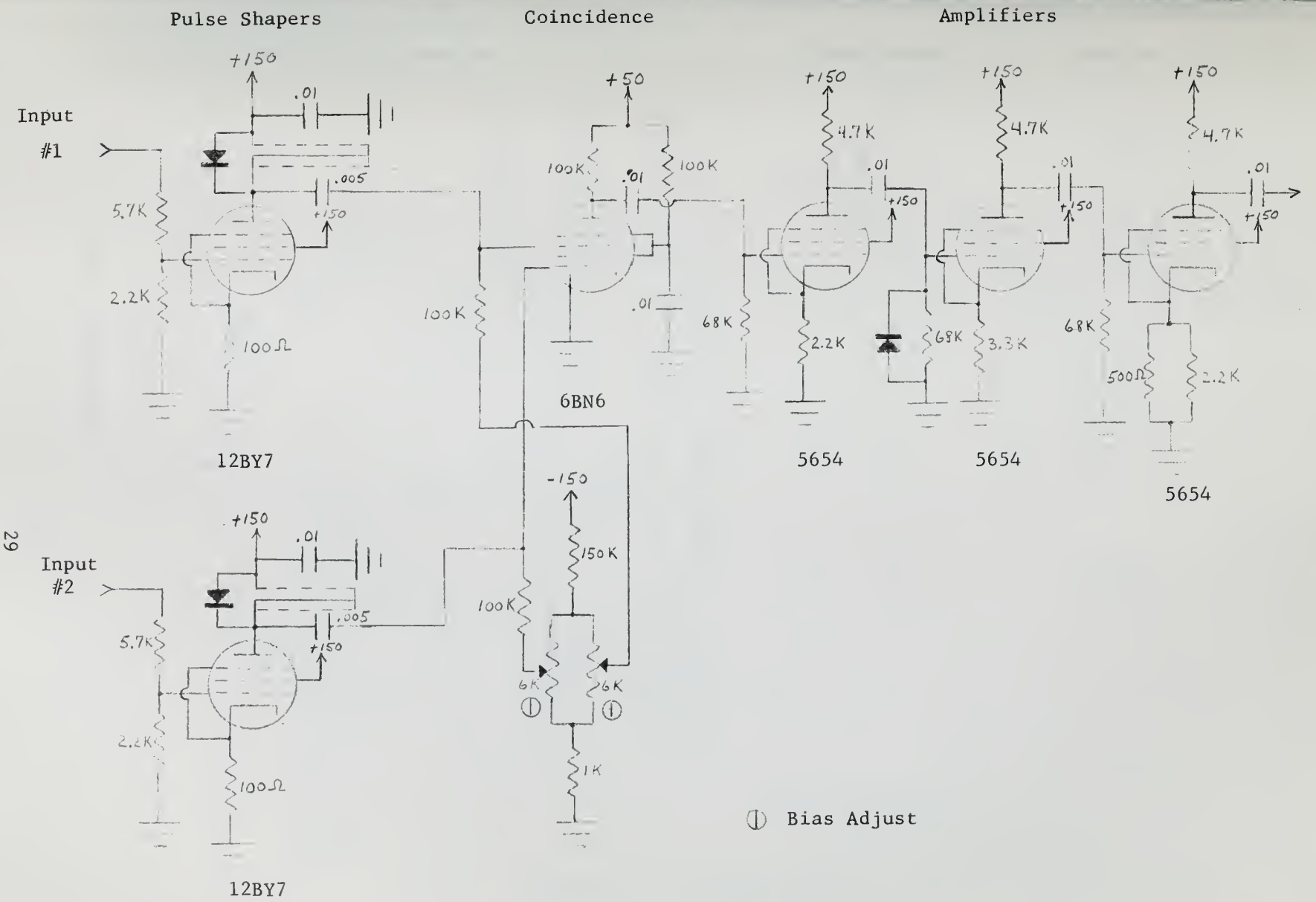

Figure. 10 a. Circuit Diagram of New Slow Coincidence Unit
Initial Stages

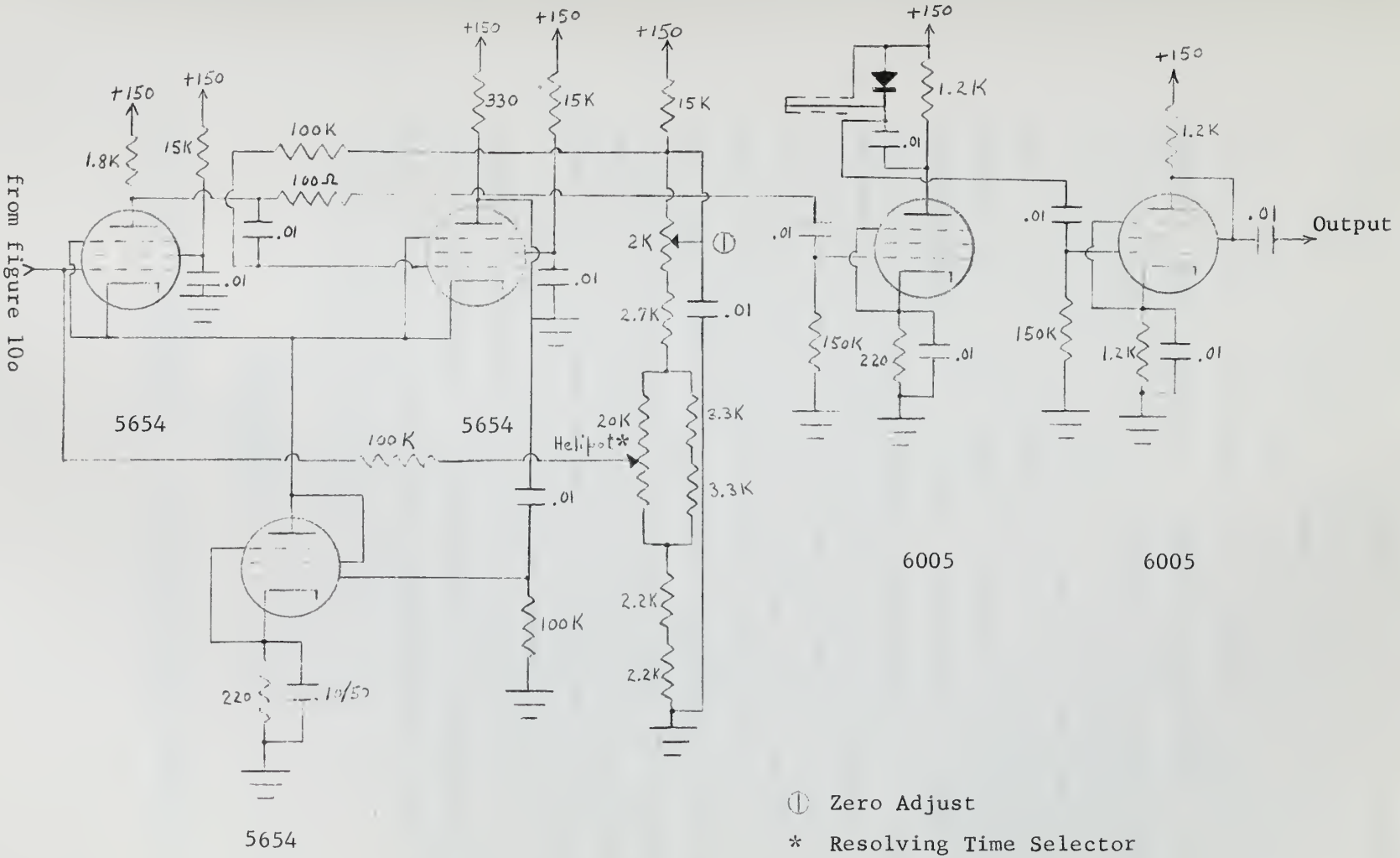

Figure 10 b. Circuit Diagram of New Slow Coincidence Unit
Final Stages

in the value of $W_{ex}(\theta_i)$ for Ni^{60} in the 105-135° region, and for future experiments with short-lived nuclides produced in the US Naval Postgraduate School Van de Graaff generator.

It was not possible to reduce the resolving time of the slow coincidence unit below a value τ_{min} which is determined by the width of the window of the differential pulse height analyzer which precedes it. This time corresponds to the difference in time between the crossing of the lower voltage discrimination level of a pulse of the lowest permissable amplitude in one channel and the time of crossing of the lower discriminator level of a simultaneous pulse of the highest permissable voltage in the second channel. Because of this irreducible minimum value for τ, and since a resolving time larger than τ_{min} gives too many accidental coincidences for an acceptable variance of the experimentally-determined correlation function, a different mode of operation was required. The scheme used consisted of adding a fast coincidence unit in parallel with the slow unit and mixing the output pulses from the two units; this scheme reduced the accidental coincidence counting rate because of the decreased τ of the fast unit, yet retained the amplitude-discriminating characteristics of the differential pulse height analyzer employed with the slow unit (Figure 11.)

The fast coincidence unit was constructed after a design by Draper and Fleischer (14) and was adjusted for a resolving time of approximately 20 nanoseconds, thus decreasing $\dot{C}_A$ by about a factor of 10 from that obtained with the slow units.

2. Relation between $\sigma\left[W_{ex}(\theta_i)\right]$ and $\sigma(\dot{C}_G)$

It is desired to minimize

$$\frac{\sigma\left[W_{ex}(\theta_i)\right]}{W_{ex}(\theta_i)} \quad . \tag{1}$$

Since $W_{ex}(\theta_i) = \left(\frac{\dot{C}_G}{\dot{N}_1 \dot{N}_2}\right)_i$ and the fractional deviations of $\dot{N}_1$

Figure 11. Block Diagram of Experimental Setup

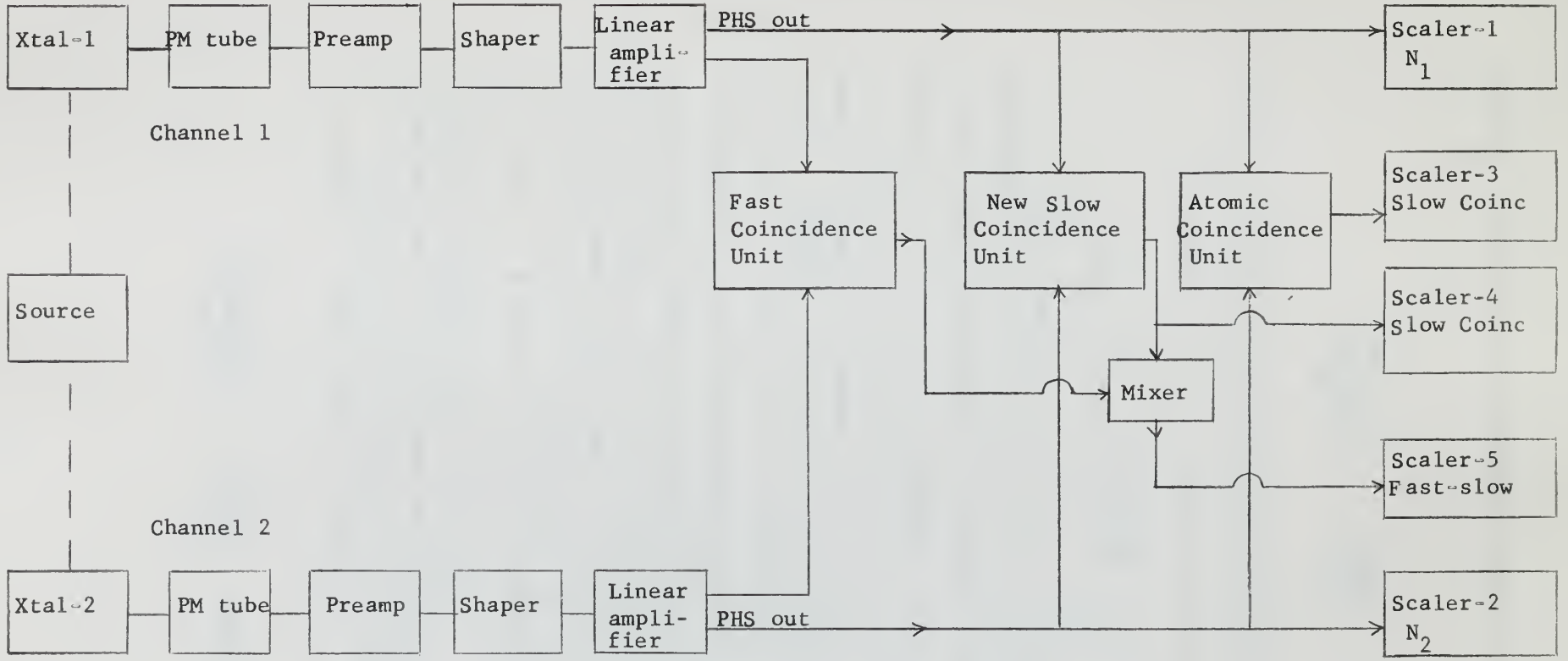

Scaler-1 Channel 1, Total Counts
2 Channel 2, Total Counts
3 Slow Coincidences Atomic Unit
4 Slow Coincidences New Unit
5 Fast-slow Coincidences (Fast & New Slow)

and $\dot{N}_2$ are very small compared to the fractional deviation of $\dot{C}_G$,

$$\frac{\sigma\left[W_{ex}(\theta_i)\right]}{W_{ex}(\theta_i)} = \frac{\sigma\left(\dot{C}_G\right)}{\dot{C}_G} \quad . \tag{12}$$

3. Effect on $\sigma^2(\dot{C}_G)$ of Decreasing the Coincidence Resolving Time

The variance of $\dot{C}_G$ is calculated from equation 11 ,

$$\sigma^2(\dot{C}_G) = \frac{\dot{C}_T}{t} + \left(\frac{\sigma_{elec}(\tau)}{\tau}\right)^2 \dot{C}_A^{\,2} + \frac{\dot{C}_A}{t} \quad .$$

It is evident from the relation $\dot{C}_A = 2\tau\dot{N}_1\dot{N}_2$ (equation 6) that decreasing the resolving time of the coincidence unit (τ) by an order of magnitude results in a similar decrease in $\dot{C}_A$. This decrease is reflected as a decrease in the third term of equation 11 by an order of magnitude since t is constant in these experiments. Assuming no change in the fractional resolving time fluctuation, $\left(\frac{\sigma_{elec}(\tau)}{\tau}\right)$, the second term of equation 11 would decrease by a factor of about 100. The genuine coincidence counting rate is independent of the coincidence unit resolving time, as long as the latter exceeds the average interval between the emissions of the two quanta; this is the case for all three coincidence units discussed in this report. Thus a decrease in $\dot{C}_A$ also results in a decrease in $\dot{C}_T$ since $\dot{C}_T = \dot{C}_A + \dot{C}_G$. This decrease in $\dot{C}_T$ results in a decrease in $\frac{\dot{C}_T}{t}$. Therefore all three terms of equation 11 decrease when τ decreases.

4. Relative Effect of Coincidence Resolving Time Drift

The previous section indicated how $\sigma^2(\dot{C}_G)$ is decreased by decreasing τ . Then from the relation

$$\frac{\sigma\left[W_{ex}(\theta_i)\right]}{W_{ex}(\theta_i)} = \frac{\sigma(\dot{C}_G)}{\dot{C}_G} \quad , \text{ equation 12,}$$

it is evident, since $\dot{C}_G$ is constant, that

$$\frac{\sigma\left[W_{ex}(0_i)\right]}{W_{ex}(0_i)}$$

has been decreased appreciably. The assumption that $\left|\frac{\sigma_{elec}(\tau)}{\tau}\right|$ did not vary was made in the last section to simplify the discussion. It is evident, however, that due to the large decreases in the values of all other terms in equation 11, including the $\dot{C}_A^2$ term which multiplies $\left|\frac{\sigma_{elec}(\tau)}{\tau}\right|$, larger values of the latter can be tolerated while still decreasing very significantly the fractional variance of $W_{ex}(0_i)$. Thus the electronic stability of the fast coincidence unit is not as critical as it would be with a unit of larger coincidence resolving time.

C. Operation of the Fast Coincidence Unit

The basic theory of operation of the fast unit and the circuitry for the Draper-Fleischer unit are given in detail elsewhere [14] and will not be repeated here.* Either single channel becomes operative when the input pulse reaches 68% of its maximum amplitude, regardless of the value of that amplitude within the range 20-100 volts. The circuit is so designed that resolving times on the order of 100 times shorter than the rise time of the input pulses can be achieved. This characteristic is required since the rise time of the pulses from the sodium iodide scintillation crystals is on the order of 200-300 nanoseconds.

Only the coincidences of 1.17 MEV and 1.33 MEV gamma-rays are of interest in this experiment with Ni^{60}. Amplitude discrimination which was performed by the differential pulse height analyzers which preceded the slow coincidence unit selected the pulses corresponding to the photopeaks of the two gamma rays. All coincidences, regardless of the pulse height, were detected by the fast unit since no amplitude discrimination preceded it. The output pulses of the slow coincidence unit and those of the fast unit were passed through a mixer circuit which effectively functioned as another coincidence unit. An output

* A block diagram of the fast unit is provided in Fig. 12.

Block Diagram, Fast Coincidence Unit

Figure 12.

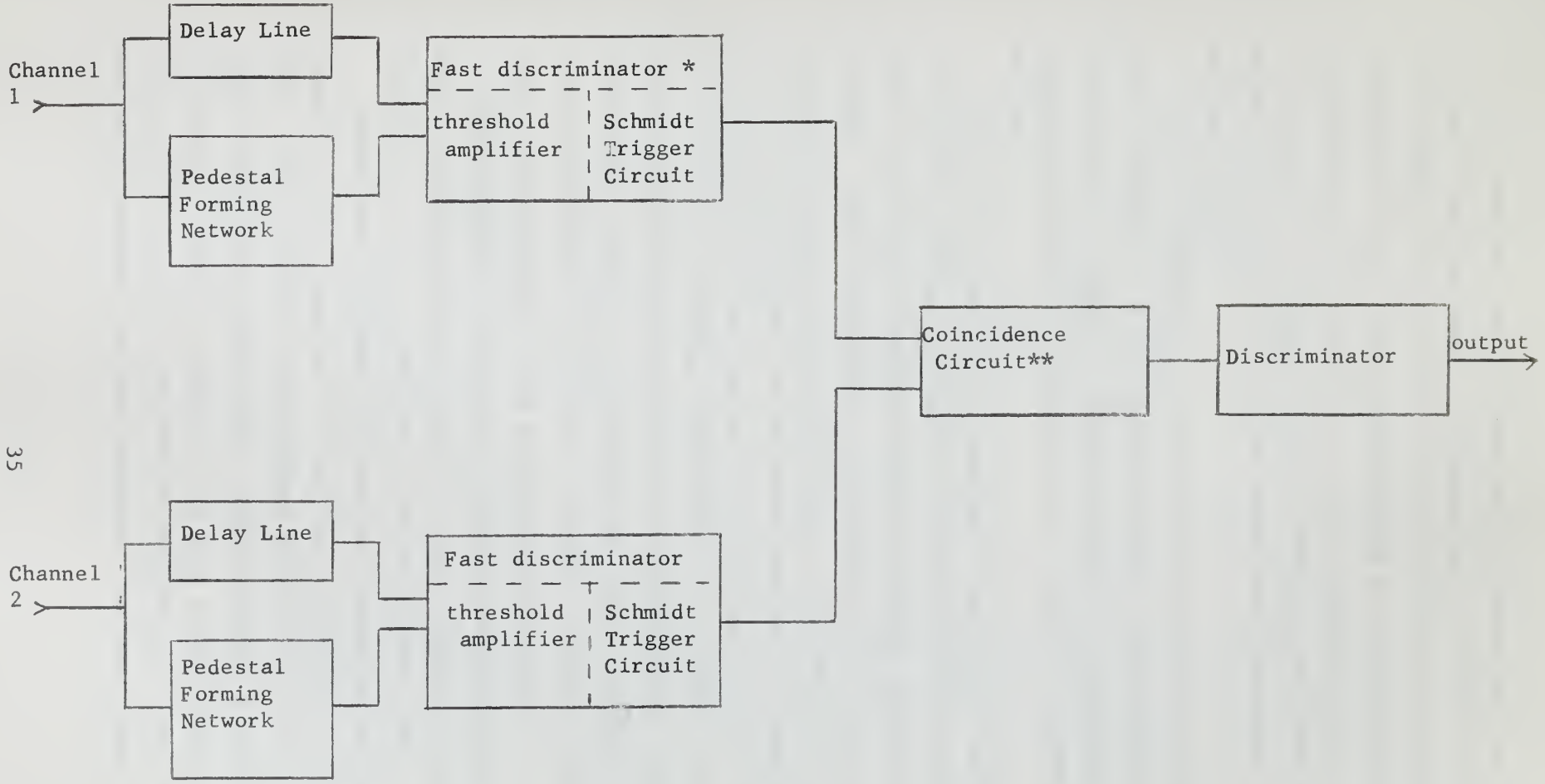

* After Farley, [15]

** After Bell & Petch & Graham, [16]

pulse was obtained from the mixer only if there was, in a time interval of about 35 microseconds, a 20-nanosecond coincidence between pulses of any height as ascertained by the fast unit and a 200-nanosecond coincidence between pulses corresponding to the photopeaks of interest as determined by the slow unit. Thus by combining these two units in this manner, an energy-selective counting system with a 20-nanosecond coincidence resolving time which was independent of the counting rate was obtained.

Certain modifications were necessary to the fast unit and are given in Figure 13. The last two stages of the Draper-Fleischer unit could not be made to function properly. This portion of the circuitry was therefore taken out, and a cathode follower was substituted.

The mixer circuit which contained circuitry for amplitude discriminating, shaping, amplifying, and mixing the fast coincidence pulse with the slow coincidence pulse was built up and tested stage-by-stage. The discriminator of the mixer unit is a uni-stable multivibrator with Zener diode stabilization. The inverter stage in the fast coincidence channel of the mixer results in a negative pulse of approximately 35-microsecond duration, the duration varying with the discriminator setting. This pulse is then mixed with a 0.7 microsecond negative pulse from the slow coincidence unit. Discrimination of the mixed output is performed by the scaler counting these fast-slow coincidences. The design of the mixer circuit is given in Fig. 14.

D. Testing and Alignment of the Fast Coincidence Unit

The alignment of the fast coincidence unit consisted of two major portions-achieving linearity in each channel, and assuring the detection of true coincidences by the coincidence stage.

Draper and Fleischer [14] describe a means of testing for linearity; i.e., ensuring that the fast discriminator fires when the input reaches the same predetermined fraction of its full amplitude, over a wide range of amplitudes. They prescribe a mercury-relay pulser delivering a five-volt negative step with a rise time of seven nanoseconds which is split, one portion triggering a 10-mc ringing circuit which provides the time reference, the other going through an

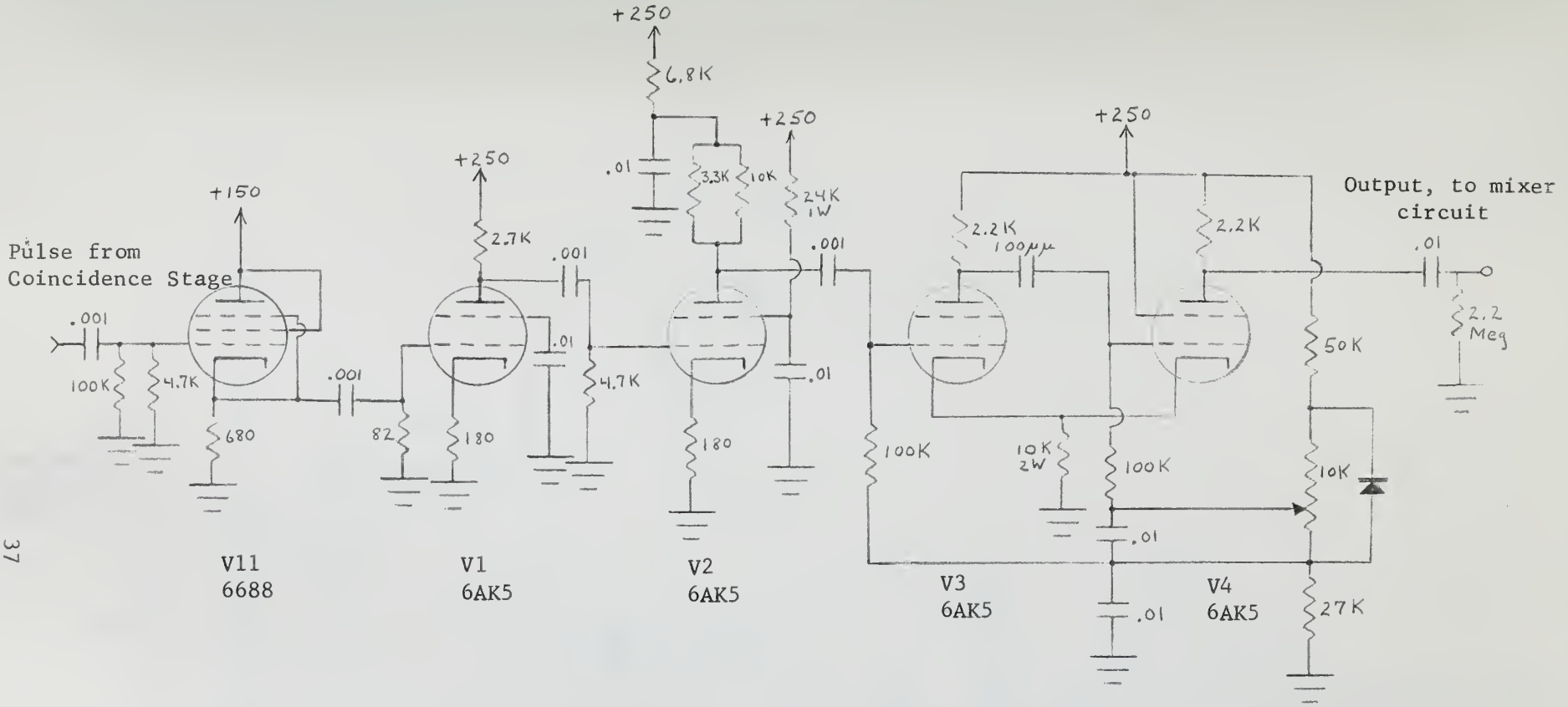

Since pulses from the fast discriminator (V9, V10 of the Draper-Fleischer circuit) are not square, it is necessary to amplitude discriminate the output of the fast coincidence unit. This is accomplished by amplifying the mixed output of the two time compensation units in V_1 and V_2 and then amplitude discriminating in the circuit comprised of V_3 and V_4. The output of V_4 then is inverted and mixed with the output of the slow coincidence unit (Figure 14).

Figure 13. Fast Coincidence Pulse Amplifying and Discriminating Circuitry

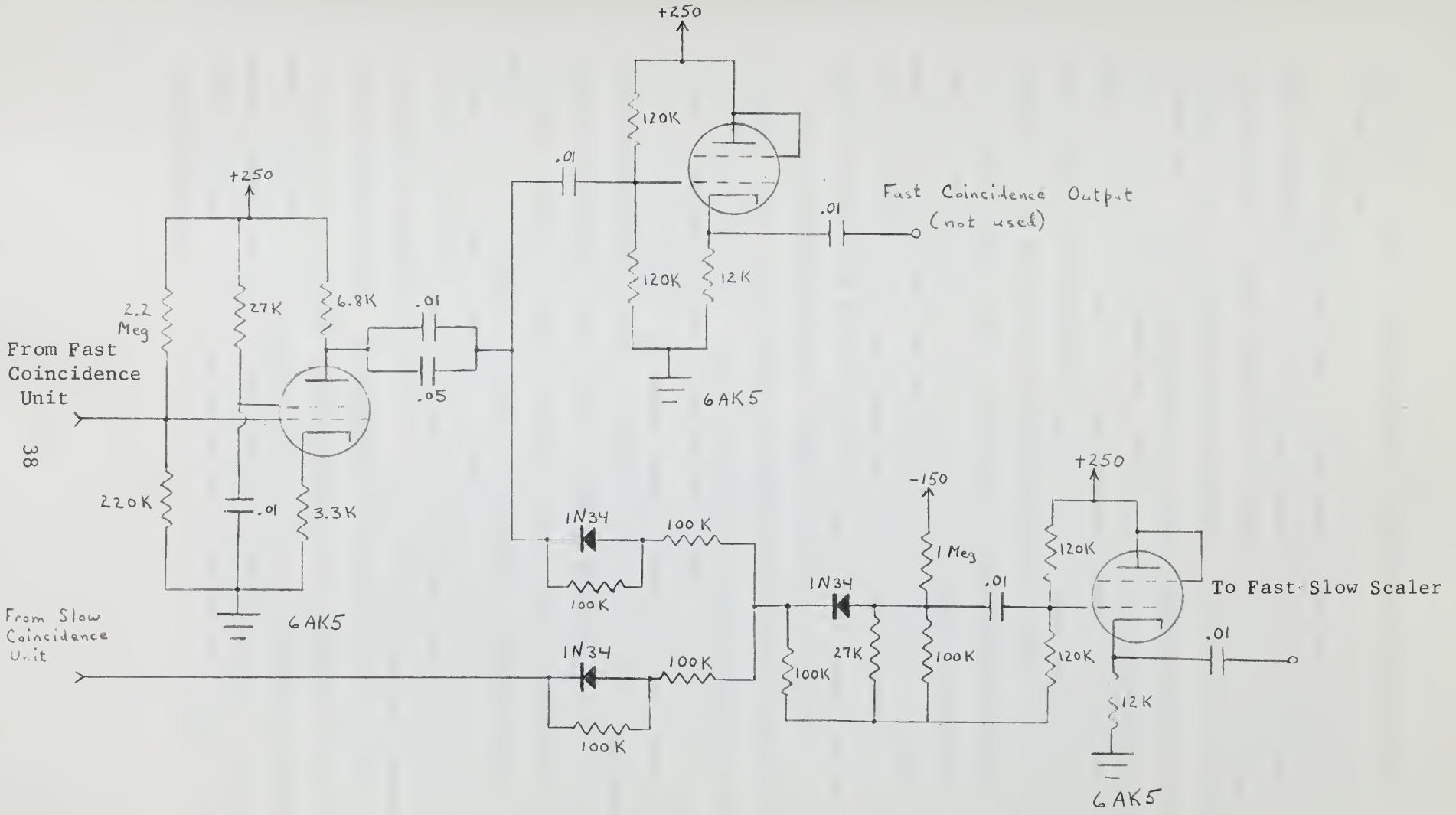

Figure 14. Circuit Diagram of Mixer Circuit

attenuator, linear pulse amplifier, and the coincidence unit (Figure 15-a).

Several modifications of this test scheme were tried, due to the nonavailability of a pulse generator which could deliver a pulse of sufficiently large amplitude and short rise time to trigger the ringing circuit satisfactorily, and due to the lack of a compensated attenuator. These modifications met with varying degrees of success. When a double pulse generator was used as a signal source, and the amplitudes of the inputs to the separate channels of the fast unit were varied by adjusting the gains of the linear amplifiers, distortion of the wave shapes resulted when the coarse gain settings were varied. This made it impractical to vary the amplitudes of the coincidence unit inputs by varying the gains of the linear amplifiers since the time reference for determining the delay within the coincidence unit itself was thus lost. Still greater wave shape distortion resulted from varying the gain of the double pulser.

The procedure which has finally emerged as workable is outlined in Figure 15-b and consists of triggering the oscilloscope with the output of the fast unit discriminators and viewing the relative delay of nuclear pulses of varied amplitudes. The problem of wave shape distortion when the coarse gain settings of the linear amplifiers were adjusted has been avoided by limiting the adjustment of delay-equivalence to the 10-volt range of amplitudes used experimentally. Since a 10-volt window is used in the differential pulse height analyzer experimentally, an equivalent time delay over this range is all that is required. The inputs to the fast unit are varied over this 10-volt range by adjusting only the fine gain controls, avoiding the distortion of wave shape which accompanies changes of the coarse gain settings. The adjustment of the fine gain controls can be avoided by providing a nuclear source or a combination of sources with different decay energies which results in different amplitude signals being received by the fast unit simultaneously. The relative delay introduced into these pulses of different amplitudes is then observable directly.

Fig. 15. Fast Coincidence Unit Test Scheme

(a) (As described by Draper and Fleischer)

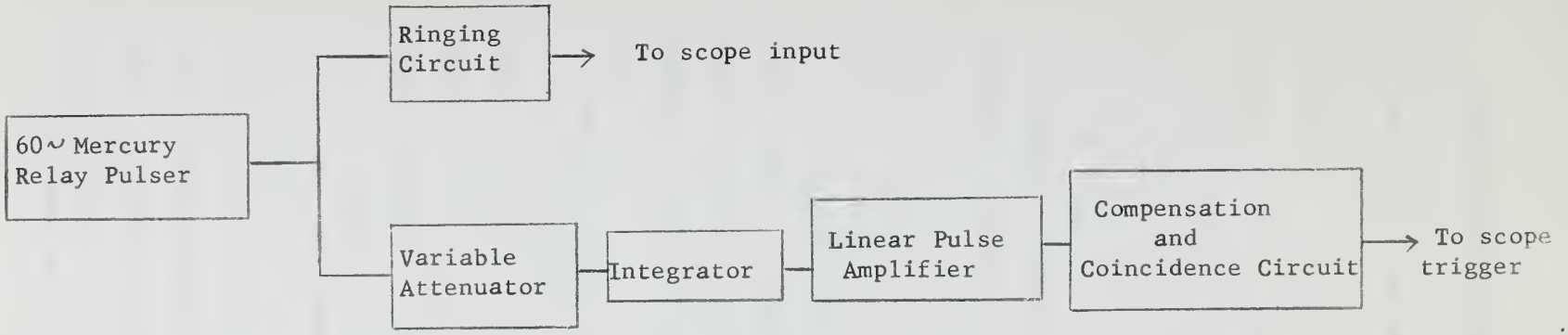

(b) As employed

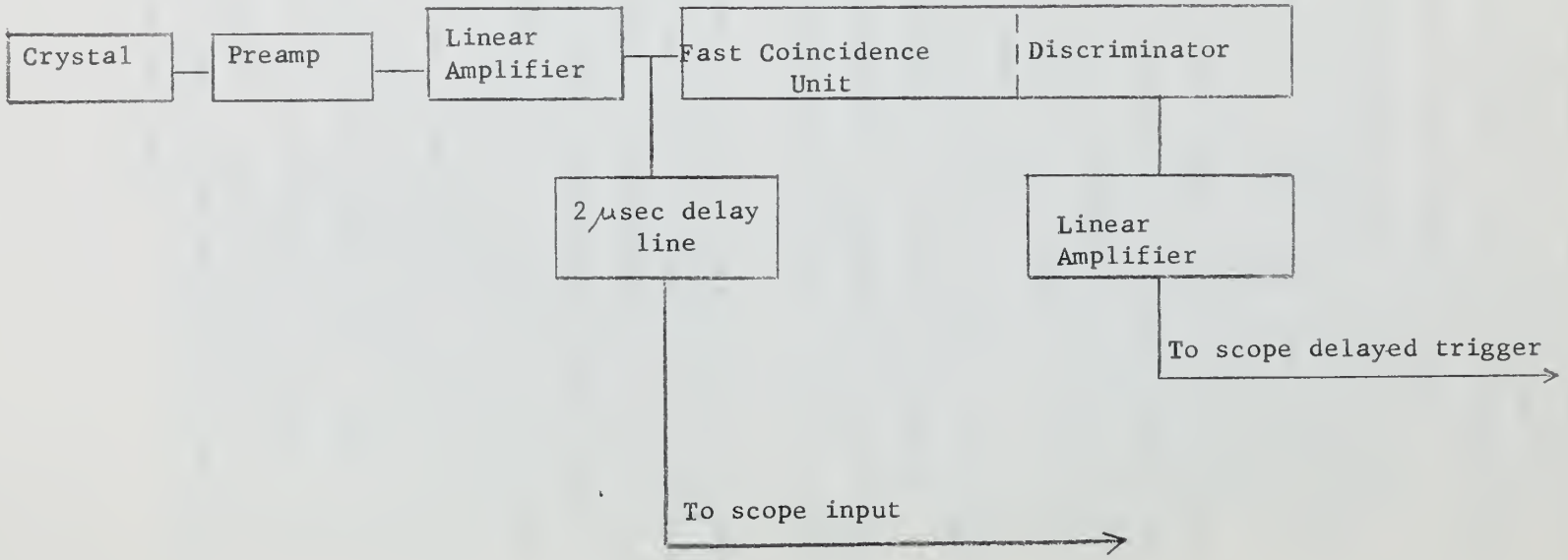

An alternate means of accomplishing this alignment consists of using test pulses from a double pulser, triggering the oscilloscope with the trigger output pulse of the double pulser and viewing the output of the fast discriminator of the fast coincidence unit in each channel. Again, the input amplitude is varied by changing the settings of the fine gain controls on the linear amplifiers.

The procedures already described ensure only that the delay which a pulse experiences as it passes through the time compensating circuit of one channel is independent of amplitude. The other major alignment requirement, which cannot be met until each channel has been aligned separately, is the assurance that the true coincidences are being detected by the unit. This requires identical total delay from the time of emission from the source through all the circuitry associated with each of the two channels and through the fast coincidence unit itself up to the coincidence stage.

To determine the ability of the fast unit to detect true coincidences before it was completely aligned, it was used in parallel with a slow unit in the angular correlation experiment in the 90-180^{o} quadrant. While it generally tracked the slow unit, it did so erratically.

Variable delay lines have been installed to facilitate the alignment for equivalent delay in the two signal channels to the coincidence stage of the fast unit. The alignment is accomplished using the experimental Co^{60} source with the experimental geometry and normalizing the total coincidence counting rate measured by the fast-slow coincidence detecting scheme to the genuine coincidence counting rate determined by the slow coincidence unit. After normalizing the total coincidence counting rate of the fast-slow combination in this manner, and making a graph of this versus the setting of the variable delay line in one of the time compensation channels of the fast unit, a plateau is obtained the width of which corresponds to the resolving time of the fast coincidence unit. The delay line is then adjusted to the center of this plateau as determined from the graph.

Thus procedures have been developed for aligning the time compensation circuit of each channel for linearity by means of either a nuclear source or a double pulser, and for aligning the two channels of the fast unit for equivalent delay by means of a nuclear source.

E. Equipment Status

The experimental equipment described herein including the new fast-slow coincidence detecting scheme is functioning well enough to be used in the experiments for which it was assembled; namely, the angular correlation of short-lived nuclides activated in the Van de Graaff generator. Due to limited unavoidable drifts in the electronic equipment, frequent checks must be made of operating characteristics, and appropriate adjustments made as necessary to ensure the closest possible control over the experimental environment. The checkout procedures which have proved extremely useful in ensuring that easily-overlooked actions are not overlooked and that checks are made in the same sequence for the greatest possible reproducibility of procedures, should be continued.

Figure 16 illustrates the layout of the major electronic portion of the experimental equipment, all rack-mounted and mobile to facilitate its use with or without the Van de Graaff generator.

Fig. 16 Electronic System

FORTRAN PROGRAM

Appendix Part A

Least Squares Analysis

```
      PROGRAM ANGCORR
      DIMENSION AN1(20,20), AN2(20,20), CT(20,20), B3(20),
     1  K(20), AND1P(20,20), AND2P(20,20), CTD(20,20), CAD(20,20),
     2  W(20,20), SW(20,20), B1(20), B2(20), SBB(20), D(20), ANISO(2)
     3  ,TAUC(20,20),STAUC(20,20),TAUD1(20,20),TAUD2(20,20), BACK1(20,20
     4 ),BACK2(20,20),T(20,20), CGD(20,20), JRUN(20,20)
      COMMON B1, B2, B3, L, ALPHA1, ALPHA2, ALPHA3, SBB
      NN = 1
    4 FORMAT(3F10.6)
    6 FORMAT(41HOGAMMA-GAMMA ANGULAR CORRELATION ANALYSIS/)
    7 FORMAT(38HONUMBER OF SETS OF DATA TO BE ANALYZED/)
      WRITE OUTPUT TAPE 4, 6
  398 FORMAT(23H023 APRIL 62 ANG CORR    )
      WRITE OUTPUT TAPE 4, 398
      WRITE OUTPUT TAPE 4, 7
    8 FORMAT (I2)
    9 FORMAT (I10)
   10 FORMAT (F12.11, 3F12.10, F7.4,  F8.4, F9.2)
   11 FORMAT(F6.2, I10)
   12 FORMAT (F9.1, F20.1, F17.1, I34)
   13 FORMAT(F10.2, I3/)
   14 READ INPUT TAPE 3, 8, MM
```

```
  500 FORMAT(I3//)
      WRITE OUTPUT TAPE 4, 500, MM



  501 FORMAT(I3)
   15 READ INPUT TAPE 3, 501, L
      READ INPUT TAPE 3, 10,CTAUC,CSTAUC,CTAUD1,CTAUD2,CBACK1,CBACK2,AT
      READ INPUT TAPE 3, 11, (B3(J), K(J), J = 1,L)
      READ INPUT TAPE 3, 4, ALPHA1, ALPHA2, ALPHA3
   16 FORMAT(16HODATA SET NUMBER/)
      WRITE OUTPUT TAPE 4, 16
      WRITE OUTPUT TAPE 4, 500, NN
C     READ OUT DATA INPUT FOR CHECK
  516 FORMAT(23HOCHECK INPUT PARAMETERS/)
      WRITE OUTPUT TAPE 4, 516
  517 FORMAT(69H0    TAUC         STAUC        TAUD1        TAUD2     BACK1
     1  BACK2      T/)
      WRITE OUTPUT TAPE 4, 517
  518 FORMAT (F13.11, 3F12.10, F7.4,  F8.4, F9.2//)
  519 WRITE OUTPUT TAPE 4,518,CTAUC,CSTAUC,CTAUD1,CTAUD2,CBACK1,CBACK2,
     1  AT
```

```
520 FORMAT(71HOTHEORETICAL LEGENDRE POLYNOMIAL COEFFICIENTS CORRECTED
   1FOR SOLID ANGLE//,3F12.6/)
    WRITE OUTPUT TAPE 4, 520, ALPHA1, ALPHA2, ALPHA3
521 FORMAT(29HONUMBER OF RUNS AT EACH ANGLE/)
    WRITE OUTPUT TAPE 4, 521
    WRITE OUTPUT TAPE 4, 13, (B3(J), K(J), J = 1, L)
    DO 18 J = 1, L
    II = 1
 17 READ INPUT TAPE 3, 12, AN1(II,J), AN2(II,J), CT(II,J),JRUN(II,J)
    READ INPUT TAPE 3, 10, TAUC(II,J), STAUC(II,J), TAUD1(II,J),TAUD2(
   1 II,J), BACK1(II,J), BACK2(II,J), T(II,J)
399 IF(TAUC(II,J)-0.0)400,400,401
400 TAUC(II,J) = CTAUC
401 IF(STAUC(II,J)-0.0) 402,402,403
402 STAUC(II,J) = CSTAUC
403 IF(TAUD1(II,J)-0.0)404,404,405
404 TAUD1(II,J) = CTAUD1
405 IF(TAUD2(II,J)-0.0)406,406,407
406 TAUD2(II,J) = CTAUD2
407 IF(BACK1(II,J)-0.0)408,408,409


408 BACK1(II,J) = CBACK1
```

```
409 IF(BACK2(II,J)-0.0)410,410,411
410 BACK2(II,J) = CBACK2
411 IF(T(II,J)-0.0)412,412,413
412 T(II,J) = AT
413 II = II+1
    IF (II-K(J)) 17, 17, 18
 18 CONTINUE
 19 FORMAT(56HOCHECK DATA INPUT OF N1, N2, AND CT AND INPUT PARAMETERS
   1/)
    WRITE OUTPUT TAPE 4, 19
528 FORMAT(9HOANGLE-   , F6.2/)
    JJ=1
529 WRITE OUTPUT TAPE 4, 528, B3(JJ)
 20 FORMAT(115HO   N1           N2           CT        TAUC          STAU
   1C       TAUD1        TAUD2     BACK1   BACK2       T          RUN /)
 21 FORMAT(F10.1,F12.1,F11.1,F13.11,3F12.10,F7.4,F8.4,F9.2,I9)
    WRITE OUTPUT TAPE 4, 20
    II = 1
530 WRITE OUTPUT TAPE 4, 21,  AN1(II,JJ), AN2(II,JJ), CT(II,JJ),TAUC(I
   1I,JJ),STAUC(II,JJ),TAUD1(II,JJ),TAUD2(II,JJ),BACK1(II,JJ),BACK2(II
  ·2 ,JJ),T(II,JJ), JRUN(II,JJ)
    IF(II-K(JJ)) 531,532,532
531 II=II+1
    GO TO 530
```

```
  532 FORMAT(5H0    /)
      WRITE OUTPUT TAPE 4, 532
      IF(JJ-L)533,534,534
  533 JJ=JJ+1
      GO TO 529
C     COMPUTE NDOT1, NDOT2, CTDOT, W AND SIGMA W FOR EACH RUN
  534 FORMAT (20HORESULTS OF ANALYSIS/)
      WRITE OUTPUT TAPE 4, 534
      JJ = 1
   25 II=1
   30 AND1P(II,JJ) = AN1(II,JJ)/T(II,JJ)*(1.0+TAUD1(II,JJ)*AN1(II,JJ)/T
     1 (II,JJ))

      AND2P(II,JJ) = AN2(II,JJ)/T(II,JJ)*(1.0+TAUD2(II,JJ)*AN2(II,JJ)/T
     1 (II,JJ))
      CTD(II,JJ) = CT(II,JJ)/T(II,JJ)
      CAD(II,JJ) = 2.0*TAUC(II,JJ)*AND1P(II,JJ)*AND2P(II,JJ)
      CGD(II,JJ) = CTD(II,JJ) - CAD(II,JJ)
      W(II,JJ) = (CTD(II,JJ)-CAD(II,JJ))/((AND1P(II,JJ)-BACK1(II,JJ))
     1 *(AND2P(II,JJ)-BACK2(II,JJ)))
      SW(II,JJ) = W(II,JJ)*SQRTF((CTD(II,JJ)/T(II,JJ)+(CAD(II,JJ)/T(II,J
     1 J)) + (STAUC(II,JJ)*CAD(II,JJ)/TAUC(II,JJ))**2))/(CTD(II,JJ)-CAD
```

```
     2 (II,JJ))
       IF (II-K(JJ)) 35, 40, 40
    35 II = II+1
       GO TO 30
    40 IF (JJ-L) 45, 50, 50
    45 JJ = JJ+1
       GO TO 25
C      COMPUTE MEAN VALUES OF W, SIGMA W, AND RMS SIGMA FOR EACH ANGLE
    50 JJ = 1
    55 SUM1 = 0.0
       SUM2 = 0.0
       II = 1
    60 SUM1 = SUM1+W(II,JJ)/(SW(II,JJ)**2)
       SUM2 = SUM2+1.0/(SW(II,JJ)**2)
       IF (II-K(JJ)) 65, 70, 70
    65 II = II+1
       GO TO 60
    70 B1(JJ) = SUM1/SUM2
       B2(JJ) = SQRTF(1.0/SUM2)
       SUM3 = 0.0
       II = 1
    71 SUM3 = SUM3+(W(II,JJ)-B1(JJ))**2
       IF (II-K(JJ)) 72, 73, 73
    72 II = II+1
```

```
      GO TO 71
   73 D(JJ) = K(JJ)
      SBB(JJ) = SQRTF(SUM3/((D(JJ)-1.0)*D(JJ)))
      IF (JJ-L) 75, 80, 80


   75 JJ = JJ+1
      GO TO 55
C     READ OUT RESULTS SO FAR
   80 FORMAT (118H0NDOT1PRIME          NDOT2PRIME     CTOTALDOT       CAC
     1CDOT      CGENDOT              W                    SIGMAW      RUN  //
     2)
   82 FORMAT (F10.4,F20.4,2F13.4,F14.4,2E20.5,I5)
      WRITE OUTPUT TAPE 4, 80
      DO 87 J= 1,L
   84 FORMAT(9H0ANGLE-   , F6.2/)
      WRITE OUTPUT TAPE 4, 84, B3(J)
      II = 1
   85 WRITE OUTPUT TAPE 4, 82, AND1P(II,J), AND2P(II,J), CTD(II,J),
     1  CAD(II,J), CGD(II,J), W(II,J), SW(II,J), JRUN(II,J)
      II = II+1
      IF (II-K(J)) 85, 85, 87
   87 WRITE OUTPUT TAPE 4, 532
```

```
   90 FORMAT   (81HO              ANGLE              WBAR          SIG
     1MA WBAR            WBARB     /)
      WRITE OUTPUT TAPE 4, 90
   95 FORMAT (F20.2, 3E20.5/)
  100 WRITE OUTPUT TAPE 4,95,(B3(J), B1(J), B2(J), SBB(J), J=1,L)
C     START LEAST SQUARES ANALYSIS
  105 CALL LEASTSQ
  115 IF (NN - MM) 120, 125, 125
  120 NN = NN+1
      GO TO 15
  125 FORMAT(15HOEND OF PROBLEM)
      WRITE OUTPUT TAPE 4, 125
      END FILE 4
      PAUSE
      END
      SUBROUTINE LEASTSQ
      JK = 1
C     SET UP ARRAYS AND COMPUTE LEGENDRE POLYNOMIAL MATRIX
  201 DIMENSION POLY(20,3), OMEGA(20,20), PART1(3,20), CEE(3,3),
     1  CEEINV(3,3), XI(3), COEFT(3), SCOEFT(3), ARGP(20), B1(20),

     2  B2(20), B3(20), SUM7(3), ANISO(2), SBB(20)
```

```
      COMMON B1, B2, B3, L, ALPHA1, ALPHA2, ALPHA3, SBB
      WFUNCTF(A,B,C,D) = A+(B*0.25)*(3.0*COSF((2.0*D)/57.2957795)+1.0)+
     1(C*0.015625)*(35.0*COSF((4.0*D)/57.2957795) + 20.0*COSF((2.0*D)/
     2 57.2957795) + 9.0)
      DO 203 I=1,L
      ARGP(I) = COSF((B3(I)/57.2957795))
      POLY(I,1) = 1.0
      POLY(I,2) = 0.5*(3.0*(ARGP(I)**2)-1.0)
  203 POLY(I,3) = 0.125*(35.0*(ARGP(I)**4)-30.0*(ARGP(I)**2)+3.0)
      IF(JK-1)206,206,204
  204 DO 205 I = 1,L
      POLY(I,1) = 1.0
      POLY(I,2) = ARGP(I)**2
  205 POLY(I,3) = ARGP(I)**4
C     COMPUTE OMEGA MATRIX, PART1 MATRIX AND CEE MATRIX
  206 DO 210 I=1,L
      DO 210 J=1,L
  210 OMEGA(I,J) = 0.0
      DO 215 I = 1, L
  215 OMEGA(I,I) = ((1.0)/B2(I))**2
      DO 225 I=1,3
      DO 225 J=1,L
      SUM5 =0.0
      DO 220 K=1,L
```

```
  220 SUM5 = POLY(K,I)*OMEGA(K,J)+SUM5
  225 PART1(I,J) = SUM5
      DO 235 I=1,3
      DO 235 J=1,3
      SUM6 = 0.0
      DO 230 K=1,L
  230 SUM6 = PART1(I,K)*POLY(K,J)+SUM6
  235 CEE(I,J) = SUM6
C     INVERT CEE
      DETCEE = CEE(1,1)*(CEE(2,2)*CEE(3,3)-CEE(3,2)*CEE(2,3))-CEE(2,1)*(
     1CEE(1,2)*CEE(3,3)-CEE(3,2)*CEE(1,3))+CEE(3,1)*(CEE(1,2)*CEE(2,3)-
     2CEE(2,2)*CEE(1,3))
```



```
      CEEINV(1,1)=(CEE(2,2)*CEE(3,3)-CEE(3,2)*CEE(2,3))/DETCEE
      CEEINV(1,2)=(CEE(3,2)*CEE(1,3)-CEE(1,2)*CEE(3,3))/DETCEE
      CEEINV(1,3)=(CEE(1,2)*CEE(2,3)-CEE(2,2)*CEE(1,3))/DETCEE
      CEEINV(2,1)=(CEE(3,1)*CEE(2,3)-CEE(2,1)*CEE(3,3))/DETCEE
      CEEINV(2,2)=(CEE(1,1)*CEE(3,3)-CEE(3,1)*CEE(1,3))/DETCEE
      CEEINV(2,3)=(CEE(2,1)*CEE(1,3)-CEE(1,1)*CEE(2,3))/DETCEE
      CEEINV(3,1)=(CEE(2,1)*CEE(3,2)-CEE(3,1)*CEE(2,2))/DETCEE
      CEEINV(3,2)=(CEE(3,1)*CEE(1,2)-CEE(1,1)*CEE(3,2))/DETCEE
      CEEINV(3,3)=(CEE(1,1)*CEE(2,2)-CEE(2,1)*CEE(1,2))/DETCEE
```

```
  241 FORMAT (3F20.12/)
      DO 246 I = 1,3
      SUM83 = 0.0
      DO 245 K = 1,L
  245 SUM83 = PART1(I,K)*B1(K) + SUM83
  246 XI(I) = SUM83
C     COMPUTE COEFFICIENTS AND THEIR SIGMAS, NORMALIZING TO FIRST
C     COEFFICIENT AND COMPUTE ANISOTROPY
      DO 248 I = 1, 3
      SUM81 = 0.0
      DO 247 K = 1, 3
  247 SUM81 = CEEINV(I,K)*XI(K) + SUM81
  248 COEFT(I) = SUM81
      DIV = COEFT(1)
      DO 249 I = 1, 3
  249 COEFT(I) = COEFT(I)/DIV
      DO 260 I=1,3
  260 SCOEFT(I) = SQRTF(CEEINV(I,I))/DIV
      ANISO(2) = COEFT(2) + COEFT(3)
  265 IF(JK-2) 274, 340, 340
  274 ANISO(1)  = (WFUNCTF(COEFT(1), COEFT(2), COEFT(3), 180.0) -
     1 WFUNCTF(COEFT(1), COEFT(2), COEFT(3), 090.0))/WFUNCTF(COEFT(1),
     2 COEFT(2), COEFT(3), 090.0)
```

```
  275 FORMAT(71HOLEAST SQUARE FIT COEFFICIENTS OF LEGENDRE POLYNOMIALS A
     1ND THEIR SIGMAS/)
      WRITE OUTPUT TAPE 4, 275
  280 WRITE OUTPUT TAPE 4, 342, (COEFT(I), SCOEFT(I), I = 1,3)
  292 FORMAT(F9.6/)



      VEESQ1 = 0.0
      DO 293 J = 1,L
  293 VEESQ1 = (B1(J)/B2(J))**2 + VEESQ1
      VEESQ2 = 0.0
      DO 294 K = 1,3
  294 VEESQ2 = COEFT(K)*XI(K)*DIV + VEESQ2
      E = L
      EPSSQ = (VEESQ1 - VEESQ2)/(E - 3.0)
  295 FORMAT(18HOEPSILON SQUARE = , E20.6/)
      WRITE OUTPUT TAPE 4, 295, EPSSQ
      IF(B3(3)-180.0) 296, 296, 320
  296 FORMAT(45HOEXPERIMENTAL FUNCTION   THEORETICAL FUNCTION/)
C     COMPUTE POINTS ON THEORETICAL AND EXPERIMENTAL CURVES
      WRITE OUTPUT TAPE 4, 296
      SUM9 = 90.0
  300 WFUNCT = WFUNCTF(COEFT(1), COEFT(2), COEFT(3), SUM9)/WFUNCTF
```

```
     1(COEFT(1), COEFT(2), COEFT(3), 090.0)
  315 VFUNCT = WFUNCTF(ALPHA1, ALPHA2, ALPHA3, SUM9 )/WFUNCTF(ALPHA1,
     1 ALPHA2, ALPHA3, 090.0)
      WRITE OUTPUT TAPE 4, 324, SUM9, WFUNCT, VFUNCT
      SUM9 = SUM9 + 5.0
      IF (SUM9 - 180.0) 300, 300, 316
  316 FORMAT(41HONORMALIZED EXPERIMENTAL WBARS AND SIGMAS/)
      WRITE OUTPUT TAPE 4,316
 1316 FORMAT    (81H0              ANGLE              WBAR              SIG
     1MA WBAR             WBARB     /)
      WRITE OUTPUT TAPE 4, 1316
      ADIV = DIV*WFUNCTF(COEFT(1), COEFT(2), COEFT(3), 090.0)
      DO 318 J = 1,L
      AB1 = B1(J)/ADIV
      AB2 = B2(J)/ADIV
      ASBB = SBB(J)/ADIV
  317 FORMAT(F20.2, 3F20.5/)
  318 WRITE OUTPUT TAPE4, 317, B3(J), AB1, AB2, ASBB
      GO TO 336
  320 WRITE OUTPUT TAPE 4, 296
      SUM10 = 180.0
```

```
 324  FORMAT(F7.2, F10.6, F20.6/)
 325 WFUNCT = WFUNCTF(COEFT(1), COEFT(2), COEFT(3), SUM10)/WFUNCTF
    1(COEFT(1), COEFT(2), COEFT(3), 270.0)
 335 VFUNCT = WFUNCTF(ALPHA1, ALPHA2, ALPHA3, SUM10)/WFUNCTF(ALPHA1,
    1 ALPHA2, ALPHA3, 270.0)
     WRITE OUTPUT TAPE 4, 324, SUM10, WFUNCT, VFUNCT
     SUM10 = SUM10 + 5.0
     IF (SUM10 - 270.0) 325, 325, 635
 635 FORMAT(41HONORMALIZED EXPERIMENTAL WBARS AND SIGMAS/)
     WRITE OUTPUT TAPE 4,635
1635 FORMAT    (81H0                ANGLE                WBAR                SIG
    1MA WBAR              WBARB     /)
     WRITE OUTPUT TAPE 4, 1635
     ADIV = DIV*WFUNCTF(COEFT(1), COEFT(2), COEFT(3), 270.0)
     DO 637 J = 1,L
     AB1 = B1(J)/ADIV
     AB2 = B2(J)/ADIV
     ASBB = SBB(J)/ADIV
 636 FORMAT(F20.2, 3F20.5/)
 637 WRITE OUTPUT TAPE4, 636, B3(J), AB1, AB2, ASBB
 336 FORMAT(2H0  //////)
 338 JK = 2
     GO TO 201
 340 FORMAT(52H0      ANISOTROPY-P        ANISOTROPY-C        SIGMA/)
```

```
     1 9HOSIGMA = , F6.4/)
       RV1 = ((COEFT(2) + COEFT(3))/COEFT(1))**2
       PAREN1 = (SCOEFT(2)**2 + SCOEFT(3)**2 + 2.0*CEEINV(2,3)/DIV**2)/
     1   ((COEFT(2) + COEFT(3))**2)
       PAREN2 = (SCOEFT(1)/COEFT(1))**2
       PAREN3 = (-2.0/DIV**2)*((CEEINV(1,2) + CEEINV(2,3))/(COEFT(1)*
     1   (COEFT(2) + COEFT(3))))
       SANISO = SQRTF(RV1*EPSSQ*(PAREN1 + PAREN2 + PAREN3))
       WRITE OUTPUT TAPE 4, 340
       WRITE OUTPUT TAPE 4, 241, ANISO(1), ANISO(2), SANISO
   341 FORMAT(42HOCOEFFICIENTS AND SIGMAS FOR COSINE SERIES/)
       WRITE OUTPUT TAPE 4, 341
   342 FORMAT(2F10.5/)


       WRITE OUTPUT TAPE 4, 342, (COEFT(I), SCOEFT(I), I = 1,3)
       WRITE OUTPUT TAPE 4, 336
       RETURN
       END
       END
```

FORTRAN PROGRAM

Appendix Part B

Solid Angle Correction

```
      PROGRAM SOLANG
  409 FORMAT(15HOPROGRAM SOLANG/)
  410 FORMAT(82HOTHEORETICAL CORRELATION FUNCTION COEFFICIENT CORRECTION
     1S FOR FINITE SOLID ANGLE     /)
  411 FORMAT(21HOMETHOD OF M. E. ROSE/)
      WRITE OUTPUT TAPE 4, 409
      WRITE OUTPUT TAPE 4, 410
      WRITE OUTPUT TAPE 4, 411
      DIMENSION H(2),T(2),R(2),BP(2),GAMMA(2),TAU(2),AINT0(2),
     1AINT2(2),AINT4(2), DELTA(2), DELTAP(2)
      POLY0F(D) = D/D
      POLY2F(D) = 0.5*(3.0*(COSF(D)**2) - 1.0)
      POLY4F(D) = 0.125*(35.0*(COSF(D)**4) -30.0*(COSF(D)**2) +3.0)
      EPSF(A,E,C) = 1.0 - EXPF(-A*E*(1.0/COSF(C)))
      EPSPF(A,B,C,D) = 1.0 - EXPF(-A*(B*(1.0/SINF(C))-D*(1.0/COSF(C))))
      ARG0F(A,E,C) = POLY0F(C)*SINF(C)*EPSF(A,E,C)
      ARGP0F(A,B,C,D) = POLY0F(C)*SINF(C)*EPSPF(A,B,C,D)
      ARG2F(A,E,C) = POLY2F(C)*SINF(C)*EPSF(A,E,C)
      ARGP2F(A,B,C,D) = POLY2F(C)*SINF(C)*EPSPF(A,B,C,D)
      ARG4F(A,E,C) = POLY4F(C)*SINF(C)*EPSF(A,E,C)
      ARGP4F(A,B,C,D) = POLY4F(C)*SINF(C)*EPSPF(A,B,C,D)
       N = 1
```

```
210 FORMAT (4F10.6)
215 READ INPUT TAPE 3, 210, R(1), T(1), H(1), TAU(1)
    READ INPUT TAPE 3, 210, R(2), T(2), H(2), TAU(2)
220 DIV = 200.0
230 DO 405 I=1,2
    BP(I) = ATANF(R(I)/(H(I) + T(I)))
    GAMMA(I) = ATANF(R(I)/H(I))
    DELTA(I) = BP(I)/DIV
    DELTAP(I) = (GAMMA(I) - BP(I))/DIV
240 BETA = 0.0
    SUM0 = ARG0F(TAU(I), T(I), 0.0) + 4.0*ARG0F(TAU(I), T(I), DELTA(I)
   1)
250 SUM0 = SUM0 + 2.0*ARG0F(TAU(I), T(I), (BETA +2.0*DELTA(I)))+4.0*
   1ARG0F(TAU(I), T(I),(BETA+3.0*DELTA(I)))



    BETA = BETA + 2.0*DELTA(I)
    IF ((BETA + 3.0*DELTA(I)) - BP(I))250,250,260
260 SUM0 = SUM0 + ARG0F(TAU(I), T(I), BP(I))
    SUMP0 = ARGP0F(TAU(I), R(I), BP(I), H(I)) +4.0*ARGP0F(TAU(I),
   1R(I), BP(I)+DELTAP(I), H(I))
    BETA = BP(I) + 2.0*DELTAP(I)
```

```
270 SUMP0 = SUMP0 +2.0*ARGP0F(TAU(I), R(I), BETA, H(I)) +4.0*ARGP0F
   1(TAU(I), R(I), BETA +DELTAP(I), H(I))
    BETA = BETA + 2.0*DELTAP(I)
    IF ((BETA + DELTAP(I)) - GAMMA(I))270,270,280
280 SUMP0 = SUMP0 + ARGP0F(TAU(I), R(I), GAMMA(I), H(I))
290 AINT0(I) = (DELTA(I)/3.0)*SUM0 + (DELTAP(I)/3.0)*SUMP0
300 BETA = 0.0
    SUM2 = ARG2F(TAU(I), T(I), 0.0) + 4.0*ARG2F(TAU(I), T(I), DELTA(I)
   1)
310 SUM2 = SUM2 + 2.0*ARG2F(TAU(I), T(I), (BETA +2.0*DELTA(I)))+4.0*
   1ARG2F(TAU(I), T(I),(BETA+3.0*DELTA(I)))
    BETA = BETA + 2.0*DELTA(I)
    IF ((BETA + 3.0*DELTA(I)) - BP(I))310,310,320
320 SUM2 = SUM2 + ARG2F(TAU(I), T(I), BP(I))
    SUMP2 = ARGP2F(TAU(I), R(I), BP(I), H(I)) +4.0*ARGP2F(TAU(I),
   1R(I), BP(I)+DELTAP(I), H(I))
    BETA = BP(I) + 2.0*DELTAP(I)
330 SUMP2 = SUMP2 +2.0*ARGP2F(TAU(I), R(I), BETA, H(I)) +4.0*ARGP2F
   1(TAU(I), R(I), BETA +DELTAP(I), H(I))
    BETA = BETA + 2.0*DELTAP(I)
    IF ((BETA + DELTAP(I)) - GAMMA(I))330,330,340
340 SUMP2 = SUMP2 + ARGP2F(TAU(I), R(I), GAMMA(I), H(I))
350 AINT2(I) = (DELTA(I)/3.0)*SUM2 + (DELTAP(I)/3.0)*SUMP2
```

```
360 BETA = 0.0
    SUM4 = ARG4F(TAU(I), T(I), 0.0) + 4.0*ARG4F(TAU(I), T(I), DELTA(I)
   1)
370 SUM4 = SUM4 + 2.0*ARG4F(TAU(I), T(I), (BETA +2.0*DELTA(I)))+4.0*
   1ARG4F(TAU(I), T(I),(BETA+3.0*DELTA(I)))
    BETA = BETA + 2.0*DELTA(I)
    IF ((BETA + 3.0*DELTA(I)) - BP(I))370,370,380
380 SUM4 = SUM4 + ARG4F(TAU(I), T(I), BP(I))



    SUMP4 = ARGP4F(TAU(I), R(I), BP(I), H(I)) +4.0*ARGP4F(TAU(I),
   1R(I), BP(I)+DELTAP(I), H(I))
    BETA = BP(I) + 2.0*DELTAP(I)
390 SUMP4 = SUMP4 +2.0*ARGP4F(TAU(I), R(I), BETA, H(I)) +4.0*ARGP4F
   1(TAU(I), R(I), BETA +DELTAP(I), H(I))
    BETA = BETA + 2.0*DELTAP(I)
    IF ((BETA + DELTAP(I)) - GAMMA(I))390,390,400
400 SUMP4 = SUMP4 + ARGP4F(TAU(I), R(I), GAMMA(I), H(I))
405 AINT4(I) = (DELTA(I)/3.0)*SUM4 + (DELTAP(I)/3.0)*SUMP4
    ANORM= 1.0/(AINT0(1)*AINT0(2))
    AQ2 =ANORM*AINT2(1)*AINT2(2)
    AQ4 =ANORM*AINT4(1)*AINT4(2)
412 FORMAT(17HOINPUT PARAMETERS/)
```

```
413 FORMAT(89H0CRYSTAL NUMBER    RADIUS    THICKNESS    DISTANCE TO SO
   1URCE    LINEAR ABSORPTION COEFF      /)
414 FORMAT(I9, F16.6, F13.6, F17.6, F21.6/)
415 FORMAT(8HORESULTS/)
420 FORMAT(6H0Q2 = F9.6/)
430 FORMAT(6H0Q4 = F9.6/)
440 FORMAT(30H0END OF PROGRAM SOLANG RESULTS/)
    WRITE OUTPUT TAPE 4, 412
    WRITE OUTPUT TAPE 4, 413
    WRITE OUTPUT TAPE 4, 414, (I, R(I), T(I), H(I), TAU(I), I = 1,2)
    WRITE OUTPUT TAPE 4, 415
    WRITE OUTPUT TAPE 4, 420, AQ2
445 WRITE OUTPUT TAPE 4, 430, AQ4
    N = N+ 1
    IF (N-17) 215,215,520
520 WRITE OUTPUT TAPE 4, 440
    END FILE 4
    PAUSE
    END
    END
```

FORTRAN PROGRAM

Appendix Part C

Coincidence Resolving Time Program

```
      PROGRAM CRTIME                                                    1
      DIMENSIONAN1(500),AN2(500), CT(500), TAUD1(500), TAUD2(500),      2
     1  T(500), TAUC(500), STAUC(500),NRUN(500)                         3
  398 FORMAT(23H026 APR CRTIME MOD      )
      WRITE OUTPUT TAPE 4, 398
   40 FORMAT (I3)                                                       3.1
   45 READ 40, MM                                                       3.2
      LM = 1                                                            3.3
   50 FORMAT(I3)                                                        4
      READ 50, L                                                        4.1
   60 FORMAT(3F12.1, 2F12.9, F10.1, I10)                                5
      READ 60,(AN1(K),AN2(K), CT(K), TAUD1(K), TAUD2(K), T(K),NRUN(K),K=6
     11,L)
      DO 70  K=1,L                                                      7
      ANDOT1 = AN1(K)/T(K)                                              8
      ANDOT1P = ANDOT1*(1.0 + TAUD1(K)*ANDOT1)                          9
      ANDOT2 = AN2(K)/T(K)                                              10
      ANDOT2P = ANDOT2*(1.0 + TAUD2(K)*ANDOT2)                          11
      TAUC(K) = (CT(K)/T(K))/(2.0*ANDOT1P*ANDOT2P)                      12
   70 STAUC(K) = TAUC(K)/SQRTF(CT(K))                                   13
      SUM1 = 0.0                                                        14
      DO 71 K = 1, L
   71 SUM1 = SUM1 + TAUC(K)/(STAUC(K)**2)                               5
      SUM2 = 0.0                                                        16
      DO 72 K = 1, L
```

```
 72 SUM2 = SUM2 + 1.0/(STAUC(K)**2)                                    7
    TAUCM= SUM1/SUM2                                                  18
    D = L                                                             19
    STAUCM = SQRTF(1.0/SUM2)                                          20
 90 FORMAT(29H0 COINCIDENCE RESOLVING TIMES/)                         21
    WRITE OUTPUT TAPE 4, 90                                           22
100 FORMAT(31H0TAU AND SIGMA TAU FOR EACH RUN/)                       23
    WRITE OUTPUT TAPE 4, 100                                          24
110 FORMAT (9P2F20.5, I10)                                            25
    WRITE OUTPUT TAPE 4, 110,(TAUC(K), STAUC(K),NRUN(K), K=1,L)
120 FORMAT(57H0MEAN RESOLVING TIME        STD DEV              RMS ERRO27
   1R/)                                                               27.1
    SUM3 = 0.0                                                        28
    DO 130  K = 1, L                                                  29
130 SUM3 = SUM3 + ((TAUC(K)-TAUCM)/STAUC(K))**2                       30
    RMS = SQRTF(SUM3/SUM2)                                            31
    WRITE OUTPUT TAPE 4, 120                                          32
140 FORMAT (9P3F20.5)                                                 33
    WRITE OUTPUT TAPE4, 140, TAUCM,STAUCM,RMS                         34
150 LM = LM + 1                                                       34.01
    IF(LM - MM) 50, 50, 160                                           34.02
160 END FILE 4                                                        34.1
    PAUSE                                                             35
    END                                                               36
    END                                                               37
```

FORTRAN PROGRAM

Appendix Part D

Results of Analysis by the Least Squares Program

```
..JOB PHELPS
GAMMA-GAMMA ANGULAR CORRELATION ANALYSIS

10 MAY VAA 11/18/
NUMBER OF SETS OF DATA TO BE ANALYZED
 2

DATA SET NUMBER
 1

CHECK INPUT PARAMETERS

    TAUC         STAUC        TAUD1        TAUD2     BACK1    BACK2      T
.00000025786 .0000000028 .0000035000 .0000035000 3.8000   3.5700   7200.00

THEORETICAL LEGENDRE POLYNOMIAL COEFFICIENTS CORRECTED FOR SOLID ANGLE
   1.000000      .099615      .008368

NUMBER OF RUNS AT EACH ANGLE
    90.00  3
   105.00  3
   120.00  3
   135.00  3
   150.00  3
   165.00  3
   180.00  3
```

CHECK DATA INPUT OF N1, N2, AND CT AND INPUT PARAMETERS

ANGLE- 90.00

N1	N2	CT	TAUC	STAUC	TAUD1	TAUD2	BACK1	BACK2	T
7715372.0	8493912.0	10525.0	.00000025786	.0000000028	.0000035000	.0000035000	3.8000	3.5700	7200.00
7695190.0	8483583.0	10214.0	.00000025786	.0000000028	.0000035000	.0000035000	3.8000	3.5700	7200.00
7676042.0	8421415.0	10118.0	.00000025786	.0000000028	.0000035000	.0000035000	3.8000	3.5700	7200.00

ANGLE- 105.00

N1	N2	CT	TAUC	STAUC	TAUD1	TAUD2	BACK1	BACK2	T
7712620.0	8520243.0	10344.0	.00000025786	.0000000028	.0000035000	.0000035000	3.8000	3.5700	7200.00
7735075.0	8543918.0	10432.0	.00000025786	.0000000028	.0000035000	.0000035000	3.8000	3.5700	7200.00
7759638.0	8556720.0	10485.0	.00000025786	.0000000028	.0000035000	.0000035000	3.8000	3.5700	7200.00

ANGLE- 120.00

N1	N2	CT	TAUC	STAUC	TAUD1	TAUD2	BACK1	BACK2	T
7696778.0	8545595.0	10420.0	.00000025786	.0000000028	.0000035000	.0000035000	3.8000	3.5700	7200.00
7701444.0	8523666.0	10422.0	.00000025786	.0000000028	.0000035000	.0000035000	3.8000	3.5700	7200.00
7744192.0	8534320.0	10571.0	.00000025786	.0000000028	.0000035000	.0000035000	3.8000	3.5700	7200.00

ANGLE- 135.00

N1	N2	CT	TAUC	STAUC	TAUD1	TAUD2	BACK1	BACK2	T
7711775.0	8522919.0	10745.0	.00000025786	.0000000028	.0000035000	.0000035000	3.8000	3.5700	7200.00
7796272.0	8552850.0	10781.0	.00000025786	.0000000028	.0000035000	.0000035000	3.8000	3.5700	7200.00
7760244.0	8476438.0	10822.0	.00000025786	.0000000028	.0000035000	.0000035000	3.8000	3.5700	7200.00

ANGLE- 150.00

N1	N2	CT	TAUC	STAUC	TAUD1	TAUD2	BACK1	BACK2	T
7665166.0	8540160.0	10734.0	.00000025786	.0000000028	.0000035000	.0000035000	3.8000	3.5700	7200.00
7723064.0	8581780.0	11152.0	.00000025786	.0000000028	.0000035000	.0000035000	3.8000	3.5700	7200.00
7551069.0	8418299.0	10557.0	.00000025786	.0000000028	.0000035000	.0000035000	3.8000	3.5700	7200.00

ANGLE- 165.00

N1	N2	CT	TAUC	STAUC	TAUD1	TAUD2	BACK1	BACK2	T
7655554.0	8519721.0	11105.0	.00000025786	.0000000028	.0000035000	.0000035000	3.8000	3.5700	7200.00
7726060.0	8546518.0	11214.0	.00000025786	.0000000028	.0000035000	.0000035000	3.8000	3.5700	7200.00
7663836.0	8565178.0	11203.0	.00000025786	.0000000028	.0000035000	.0000035000	3.8000	3.5700	7200.00

ANGLE- 180.00

N1	N2	CT	TAUC	STAUC	TAUD1	TAUD2	BACK1	BACK2	T
7716070.0	8530187.0	11177.0	.00000025786	.0000000028	.0000035000	.0000035000	3.8000	3.5700	7200.00
7724981.0	8524972.0	11083.0	.00000025786	.0000000028	.0000035000	.0000035000	3.8000	3.5700	7200.00
7713354.0	8583727.0	11206.0	.00000025786	.0000000028	.0000035000	.0000035000	3.8000	3.5700	7200.00

RESULTS OF ANALYSIS

NDOT1PRIME	NDOT2PRIME	CTOTALDOT	CACCDOT	CGENDOT	W	SIGM
ANGLE- 90.00						
1075.5984	1184.5810	1.4618	.6571	.8047	.63573E-06	.14678
1072.7744	1183.1346	1.4186	.6546	.7640	.60594E-06	.14590
1070.0951	1174.4292	1.4053	.6481	.7571	.60645E-06	.14654
ANGLE- 105.00						
1075.2133	1188.2683	1.4367	.6589	.7778	.61275E-06	.14575
1078.3555	1191.5838	1.4489	.6627	.7862	.61587E-06	.14551
1081.7927	1193.3766	1.4562	.6658	.7905	.61630E-06	.14523
ANGLE- 120.00						
1072.9966	1191.8187	1.4472	.6595	.7877	.62001E-06	.14596
1073.6495	1188.7477	1.4475	.6582	.7893	.62249E-06	.14618
1079.6313	1190.2397	1.4682	.6627	.8055	.63093E-06	.14607
ANGLE- 135.00						
1075.0951	1188.6431	1.4924	.6590	.8333	.65638E-06	.14736
1086.9193	1192.8347	1.4974	.6686	.8287	.64336E-06	.14597
1081.8775	1182.1340	1.5031	.6596	.8435	.66386E-06	.14759
ANGLE- 150.00						
1068.5732	1191.0575	1.4908	.6564	.8345	.65996E-06	.14775
1076.6748	1196.8862	1.5489	.6646	.8843	.69071E-06	.14810
1052.6092	1173.9929	1.4662	.6373	.8289	.67528E-06	.15022

ANGLE- 165.00

1067.2283	1188.1952	1.5424	.6540	.8884	.70520E-06	.14966
1077.0940	1191.9479	1.5575	.6621	.8954	.70201E-06	.14875
1068.3871	1194.5611	1.5560	.6582	.8978	.70808E-06	.14935

ANGLE- 180.00

1075.6961	1189.6609	1.5524	.6600	.8924	.70191E-06	.14895
1076.9430	1188.9306	1.5393	.6603	.8790	.69098E-06	.14852
1075.3161	1197.1589	1.5564	.6639	.8925	.69783E-06	.14842

ANGLE	WBAR	SIGMA WBAR	WBARB
90.00	.61599E-06	.84528E-08	.98458E-08
105.00	.61498E-06	.84003E-08	.11189E-08
120.00	.62448E-06	.84334E-08	.33054E-08
135.00	.65445E-06	.84853E-08	.59896E-08
150.00	.67530E-06	.85840E-08	.88763E-08
165.00	.70509E-06	.86172E-08	.17529E-08
180.00	.69690E-06	.85812E-08	.31886E-08

LEAST SQUARE FIT COEFFICIENTS OF LEGENDRE POLYNOMIALS AND THEIR SIGMAS

1.00000	.00565
.09200	.01024
.00991	.01239

EPSILON SQUARE = .644725E+00

EXPERIMENTAL FUNCTION		THEORETICAL FUNCTION
90.00	1.000000	1.000000
95.00	1.000802	1.000943
100.00	1.003216	1.003769
105.00	1.007256	1.008467
110.00	1.012936	1.015010
115.00	1.020250	1.023340
120.00	1.029152	1.033355
125.00	1.039539	1.044892
130.00	1.051232	1.057716
135.00	1.063963	1.071511
140.00	1.077377	1.085886
145.00	1.091035	1.100376
150.00	1.104433	1.114467
155.00	1.117029	1.127615
160.00	1.128273	1.139280
165.00	1.137647	1.148956
170.00	1.144698	1.156209
175.00	1.149077	1.160702
180.00	1.150562	1.162223

NORMALIZED EXPERIMENTAL WBARS AND SIGMAS

ANGLE	WBAR	SIGMA WBAR	WBARB
90.00	1.00623	.01381	.01608
105.00	1.00458	.01372	.00183
120.00	1.02010	.01378	.00540
135.00	1.06907	.01386	.00978
150.00	1.10311	.01402	.01450
165.00	1.15178	.01408	.00286
180.00	1.13840	.01402	.00521

ANISOTROPY-P	ANISOTROPY-C	SIGMA
.150562200670	.150562197679	.028830656297

COEFFICIENTS AND SIGMAS FOR COSINE SERIES

1.00000	.01053
.10529	.05816
.04527	.05658

Appendix E FORTRAN Program
Glossary of Terms for the
Least Squares Analysis

1. Check of input parameters

TAUC	Coincidence unit resolving time (sec)
STAUC	Standard deviation of τ (sec)
TAUD1	System dead time, Channel 1 (sec)
TAUD2	System dead time, Channel 2 (sec)
BACK1	Background, channel 1 (counts per sec)
BACK2	Background, channel 2 (counts per sec)
T	Duration of run (sec)

2. Check data input of $N_1 N_2$ and CT and input parameters

N_1	Total counts, channel 1
N_2	Total counts, channel 2
CT	Total coincidence counts

3. Results of analysis

NDOT1PRIME	Count rate, channel 1, corrected for system dead time and background (counts per sec) Corresponds to $\hat{N}_1$ in text
NDOT2PRIME	Same, channel 2
CTOTALDOT	$\dot{C}_T$
CACCDOT	$\dot{C}_A$
CGENDOT	$\dot{C}_G$
W	$W_{ex}(\theta_i) = \left(\frac{\dot{C}_G}{\hat{N}_1 \hat{N}_2} \right)_i$
SIGMAW	$\sigma\left[W_{ex}(\theta_i)\right] = \left[\frac{\sigma(\dot{C}_G)}{\dot{C}_G}\right] \times \left[W_{ex}(\theta_i)\right]$
WBAR	$\overline{W}_{ex}(\theta_i) = \frac{\sum_j \left(\frac{1}{\sigma^2 \left[W_{ex}(\theta_i)\right]_j} \left[W_{ex}(\theta_i)\right]_j \right)}{\sum_j \left(\frac{1}{\sigma^2 \left[W_{ex}(\theta_i)\right]_j} \right)}$

SIGMAWBAR $$\sigma\left[\bar{W}_{ex}(\theta_i)\right] = \sqrt{\frac{1}{\sum_j \left(\frac{1}{\sigma^2\left[W_{ex}(\theta_i)\right]_j} \right)}}$$

WBARB $$\bar{\sigma}\left[\bar{W}_{ex}(\theta_i)\right] = \sqrt{\frac{\sum_{j=1}^{N} \left\{ \left[W_{ex}(\theta_i)\right]_j - \bar{W}_{ex}(\theta_i) \right\}^2}{N\,(N-1)}}$$

where N is the number of runs at the angle θ_i.

EXPERIMENTAL FUNCTION $W_{ls}(\theta)$ normalized to $W_{ls}(90)$ and evaluated at 5^o intervals.

THEORETICAL FUNCTION $W_{th}(\theta)$ normalized to $W_{th}(90)$ and evaluated at 5^o intervals.

NORMALIZED EXPERIMENTAL WBARS AND SIGMAS

WBAR $W_{ex}(\theta_i)$ normalized to $W_{ls}(90)$

ANISOTROPY - P $\left[\frac{\bar{W}_{ls}(180)}{\bar{W}_{ls}(90)} - 1\right]$ based upon Legendre series representation of W_{ls}.

ANISOTROPY - C Same, based on Cosine series representation of W_{ls}.

SIGMA Standard deviation of ANISOTROPY - P

BIBLIOGRAPHY

1. D R. Hamilton, Phys Rev 58, 122 (1940)
2. D.L. Falkoff andG.E. Uhlenbeck, Phys Rev, 79, 323 (1950)
3. L.C. Biedenharn and M.E Rose, Rev of Mod Phys, 25, 729 (1953)
4. D.R. Hamilton, Phy Rev 74, 782 (1948)
5. F. Metzger and M. Deutsch, Phys Rev, 78, 551 (1950)
6. J.V. Dunworth, Rev Scien Instr, 11, 167 (1940)
7. M.E. Rose, Phys Rev, 91, 610 (1953)
8. J.S. Lawson, Jr., and H. Frauenfelder, Phys Rev, 91, 649 (1953)
9. F.A. Verser, Jr., Thesis, USNPS, (1960), unpubl
10. B.J. Conway, Thesis, USNPS, (1961) unpubl
11. E.D. Klema and F.K. McGowan, Phys Rev, 91, 616 (1953)
12. S. Colombo et al, Il Nuovo Cimento, 2, 471 (1955)
13. J.B. Garg, Nuc Instr and Meth, 6, 187 (1960)
14. J.E. Draper and A.A. Fleischer, Rev Sci Instr, 31, 49 (1960)
15. F.J.M. Farley, Rev Sci Instr, 29, 595 (1958)
16. R.E. Bell, R.L. Graham, and H.E. Petch, Canadian Jour Phys, 30, 35 (1952)